

Lockheed Electronics Company, Inc.

A SUBSIDIARY OF
LOCKHEED CORPORATION

1830 NASA Road 1, Houston, Texas 77058
Tel. 713-333-5411

7.9 - 10149

CR 15-1884

JSC-14604

(11) (11)

Ref: 642-7090
Contract NAS 9-15200
Job Order 73-743-29

(E79-10149) SEPARABILITY STUDY OF WHEAT AND
SMALL GRAINS (Lockheed Electronics Co.)
55 p HC A04/MF A01 CSCI 02C

N79-18413

Unclas
G3/43 00149

TECHNICAL MEMORANDUM

SEPARABILITY STUDY OF WHEAT AND SMALL GRAINS

By

R. K. Lenington and N. E. Marquina

"Made available under NASA sponsorship
in the interest of early and wide dis-
semination of Earth Resources Survey
Program information and without liability
for any use made thereof."

Approved By:

T. C. Minter
T. C. Minter, Supervisor
Techniques Development Section

November 1978

LEC-12581

PRECEDING PAGE BLANK NOT FILMED

CONTENTS

Section	Page
1. INTRODUCTION.	1-1
1.1 <u>BACKGROUND</u>	1-1
1.2 <u>ON-LINE PATTERN ANALYSIS AND RECOGNITION SYSTEM.</u>	1-2
1.2.1 CLASSIFICATION LOGIC DESIGN AND EVALUATION	1-3
1.2.2 LINEAR AND NONLINEAR PROJECTIONS	1-4
2. THE DATA SET.	2-1
3. SEPARABILITY ANALYSIS OF WHEAT AND OTHER SMALL GRAINS	3-1
3.1 <u>SEPARABILITY AS A FUNCTION OF CROP CALENDAR.</u>	3-1
3.2 <u>MULTITEMPORAL SEPARABILITY</u>	3-11
4. DEVELOPMENT OF ANALYST AIDS	4-1
4.1 <u>SEGMENT-DEPENDENT PROJECTION RESULTS</u>	4-1
4.2 <u>FIXED PROJECTION RESULTS</u>	4-1
5. CONCLUSIONS AND RECOMMENDATIONS	5-1
5.1 <u>CONCLUSIONS.</u>	5-1
5.2 <u>RECOMMENDATIONS.</u>	5-1
6. REFERENCES.	6-1

PRECEDING PAGE BLANK NOT FILMED

TABLES

Table		Page
2-1	SEGMENTS, LOCATION OF SEGMENTS, AND ACQUISITION DATES USED IN THE DATA SET.	2-2
3-1	THE PCC FOR SPRING WHEAT.	3-2
3-2	THE PCC FOR BARLEY.	3-12
3-3	THE PCC FOR OATS.	3-12
3-4	MULTITEMPORAL PCC'S BY CROP CLASS	3-18
4-1	COMPARISON OF PCC'S FOR G-B AND 192FISHER PROJECTION.	4-11
4-2	MEAN AND STANDARD DEVIATIONS OF G-B AND 192FISHER PROJECTIONS	4-12

PRECEDING PAGE BLANK NOT FILMED

FIGURES

Figure		Page
2-1	Eigenvector projection with boundary pixels, segment 1512 . . .	2-4
2-2	Fisher discriminant vector projection with boundary pixels, segment 1512.	2-5
2-3	Eigenvector projection without boundary pixels, segment 1512.	2-6
2-4	Fisher discriminant vector projection without boundary pixels, segment 1512.	2-7
3-1	Eigenvector projection, segment 1830, day 157	3-3
3-2	Eigenvector projection, segment 1830, day 175	3-4
3-3	Eigenvector projection, segment 1830, day 193	3-5
3-4	Eigenvector projection, segment 1830, day 211	3-6
3-5	Fisher discriminant projection, segment 1830, day 157	3-7
3-6	Fisher discriminant projection, segment 1830, day 175	3-8
3-7	Fisher discriminant projection, segment 1830, day 193	3-9
3-8	Fisher discriminant projection, segment 1830, day 211	3-10
3-9	Multitemporal Fisher discriminant vector projection, segment 1899.	3-14
3-10	Fisher discriminant vector projection, segment 1899, day 193	3-15
3-11	Multitemporal Fisher discriminant vector projection, segment 1929.	3-16
3-12	Fisher discriminant vector projection, segment 1929, day 184	3-17
3-13	Multitemporal generalized Fisher discriminant vector projection, segment 1681.	3-19
4-1	Two date generalized Fisher discriminant vector fixed projection, segment 1513.	4-6

FIGURES

Figure		Page
4-2	Two date Fisher discriminant vector fixed projection, segment 1513.	4-7
4-3	Two date generalized Fisher discriminant vector fixed projection, segment 1742.	4-8
4-4	Two date Fisher discriminant vector fixed projection, segment 1742.	4-9
4-5	Single date Fisher discriminant vector fixed projection, segment 1513.	4-13
4-6	Single date G-B projection, segment 1513.	4-14

ACRONYMS

AI	analyst-interpreter
CAMS	Classification and Mensuration Subsystem
192Fisher	results obtained by using the One-day Fisher plane
G-B	greenness-brightness
LACIE	Large Area Crop Inventory Experiment
Landsat	NASA land observatory satellite
MOOS	MULTICS OLPARS Operating System
MULTICS	The operating system for the Honeywell HIS 6180 computer
NLM	nonlinear map
NMV	nearest mean vector
OLPARS	On-Line Pattern Analysis and Recognition System
PCC	probability of correct classification
PDP-1145	Programmed Data Processor, Model 11/45
pixels	picture elements
RADC	Rome Air Development Center (at Griffis Air Force Base, N.Y.)
WPS	Waveform Processing System

1. INTRODUCTION

This study addresses the problem of analyzing the spectral separability of wheat from other small grains and developing fixed and/or segment-dependent projections to aid in the identification and labeling of wheat as opposed to other small grains in multispectral images acquired by the National Aeronautics and Space Administration land observatory satellite (Landsat). Emphasis is placed on the relation of unitemporal and multitemporal separability to the number and timing of the acquisitions used. The most important tools used in the present study are the Fisher plane, the eigenvector plane, and the generalized discriminant plane.

Section 1.1 contains a brief description of the background to this study, and section 1.2 presents an introduction to the On-Line Pattern Analysis and Recognition System (OLPARS). Section 2 defines the data sets used in this study; section 3 deals with the general results concerning separability of wheat and small grains. Sections 4.1 and 4.2 describe the different projections studied and the results in terms of proposed projections for wheat and other small-grain identification and labeling. Section 5 presents the conclusion reached in this study and the recommendations for future work.

1.1 BACKGROUND

In the 3 years in which the Large Area Crop Inventory Experiment (LACIE) has been operational, it has become increasingly clear that in order to obtain a sufficiently accurate wheat area estimate, particularly in the areas where spring wheat is grown, it would be necessary to distinguish wheat from other small grains such as barley and oats. Because the small-grain crops are so similar in their reflectance and development, it has been the practice in LACIE Phase III to simply label and classify small grains as a class. A wheat estimate was then generated by developing a ratio of wheat to other small grains based on historical and economical variables. Such a ratio was developed for each stratum separately. The problem is that these ratios are not constant from year to year and are difficult to predict accurately. In addition, it is not clear that the analyst-interpreters (AI's) are able

to identify and label all of the small-grain signatures with the same confidence with which they can label wheat. These related factors are believed to have contributed to a persistent underestimate of wheat area in the spring wheat areas of the United States.

Because of the difficulties encountered in areas where wheat and other small grains are grown together, it was decided that one of the goals for the LACIE Transition Year would be the development of techniques and procedures for labeling and classifying wheat directly. This document, which is a part of the development effort, addresses the problems of acquisition selection for maximum separability of wheat versus other small grains and the development of analyst labeling aids. The objective of this research is to develop techniques which will allow the analyst to reliably distinguish wheat from other small grains in an operational setting.

1.2 THE ON-LINE PATTERN ANALYSIS AND RECOGNITION SYSTEM (OLPARS)

Sammon (ref. 1), Kanal (ref. 2), and Simmons (ref. 3), among others, have proposed that no particular solution (among a choice of learning machines, statistical approaches, spatial filtering, heuristic programming, or formal linguistic approaches) has proven relevant to all pattern recognition problems. For several years, the Rome Air Development Center (RADC) conducted an exploratory development program to establish techniques for digital signal processing and pattern recognition. They adopted an interactive approach to the solution of pattern recognition problems, coupling a knowledgeable human problem-solver with an interactive computer graphics system. The general purpose computer contains a library of data analysis, digital signal processing, and pattern classification algorithms. Using a graphics display console, a human operator can analyze his data, and based on what he sees coupled with any prior knowledge he may possess, choose an appropriate pattern classification procedure, observe the results, and continue to iterate in this manner. Eventually, one of two things will happen: (1) he achieves an acceptable level of performance whereby the output of the computer consists of the design parameters for a classifier which can be implemented by means of special purpose software or (2) he reaches a point where

no further improvement seems possible. Hopefully, the operator gained insight as to why an acceptable level of performance was not achieved if further improvement appears impossible.

OLPARS is resident on two systems at RADC. One version is on a Programmed Data Processor, Model 11/45 (PDP-11/45) computer under the Waveform Processing System (WPS). This is a single-user system employing high performance interactive graphics, and as a module under WPS, provides for ease of interaction between the feature hypothesis mode conducted under WPS and rapid testing of these hypotheses under OLPARS.

A second version of OLPARS, the one used in the present study, is implemented on a Honeywell HIS 6180 computer under the MULTICS operating system. MULTICS is a time-sharing system that utilizes a virtual memory concept. Interactive graphics capability is provided by a Tektronix 4002A storage tube with alphanumeric keyboard, joystick, and hardcopy unit.

Both versions of OLPARS include their own executive software, filing system, display package, and software modules for feature evaluation, vector data structure analysis, measurement transformation, and classifier logic design (ref. 4). In addition, OLPARS contains quite an extensive collection of routines. More on the topic of routines follows.

1.2.1 CLASSIFICATION LOGIC DESIGN AND EVALUATION

This subsection describes some of the classifier logic available in OLPARS. These routines allow the user to tailor the decision logic design to the structure of the class data. A brief description of some of the routines used in this study follows:

- Fisher pairwise classifier logic is constructed by computing optional linear discriminants and thresholds to distinguish between every pair of classes (subclasses) within a designated group. The linear discriminant is the Fisher linear discriminant given by the following equation.

$$d_{ij} = \alpha W_{ij}^{-1} \Delta_{ij}$$

$$\Delta_{ij} = \underline{\mu}_i - \underline{\mu}_j ; W_{ij} = (N_i - 1)C_i + (N_j - 1)C_j$$

where

$\underline{\mu}_i$ = mean vector of class (subclass) i

C_i = covariance matrix for class (subclass) i

- Nearest mean vector (NMV) logic implementation provides capabilities for classification of data utilizing one of three metrics (Euclidean distance, weighted vector distance, and Mahalanobis weighted distance). An unknown vector, then, is assigned to the reference class for which the decision metric is minimized.
- Closed decision boundary logic creates an L-dimensional closed hyperregion for each of the selected data sets. An unknown vector is assigned to a class if, and only if, it lies in the hyperregion associated with that class and no other. If an unknown vector should fall into more than one hyperregion, it may be rejected or placed in a new data tree for further logic design at the user's discretion. Vectors which do not lie within any hyperregion are rejected. The three types of hyperregion available are: hyperrectangular, hyperspherical, and hyperellipsoidal.

1.2.2 LINEAR AND NONLINEAR PROJECTIONS

The basic use of projections in the MULTICS:OLPARS Operating System (MOOS) is to determine if the structure of the data for a particular class is unimodal or multimodal. If it is multimodal, it is frequently better to subdivide the class before attempting to design logic for distinguishing between classes. This is particularly true if the logic to be designed is statistically based.

All of the algorithms for structure analysis in MOOS involve projecting the data onto a one- or two- space area, and allowing the analyst to draw a partition or partitions of the space if multimodality is present. All of the projections except one, nonlinear map (NLM), are linear. The linear projections may also be used as the basis for group logic design.

The linear and nonlinear projections are:

- The eigenvector plane (least squares) is defined by any two eigenvectors of the covariance matrix. The plane defined by the first two eigenvectors has been used extensively in this study. The rationale is that this plane best fits the L-dimensional data in the least-squares sense.
- OLPARS offers the analyst another projection direction or plane. The two classes, upon which the projection is based, may be composed of any two classes of the data set, or they may be composed of any two groups of classes which are lumped together for the purpose of determining the projection direction or directions. The entire current data set is projected into the space defined by the Fisher discriminant \underline{d}_1 and a second vector, \underline{d}_2 , where \underline{d}_2 is that direction which maximizes the projected between-class scatter relative to the sum of the projected within-class scatter, under the constraint that \underline{d}_2 be orthogonal to \underline{d}_1 . In summary,

$$\underline{d}_1 = \alpha_1 W^{-1} \Delta$$

$$\underline{d}_2 = \alpha_2 \left\{ W^{-1} - \left(\Delta^T [W^{-1}]^2 \Delta / \Delta^T [W^{-1}]^3 \Delta \right) [W^{-1}]^2 \right\} \Delta$$

where

α_1 and α_2 are normalizing constants; Δ is the difference between the class mean vectors, $\mu_1 - \mu_2$; and W is the sum of the within-class scatter matrices.

If the one-space option is chosen, the data are projected on \underline{d}_1 ; that is, the Fisher direction only.

- Generalized discriminant projections offer the analyst the capability of projecting data onto a discriminant direction or plane which has been optimized to produce maximum discrimination for all classes. This is a generalization of the Fisher discriminant projection described previously.
- The Fisher discriminant is obtained by solving for the unit vector \underline{d} which maximizes the following ratio:

$$R = \frac{\underline{d}^T B \underline{d}}{\underline{d}^T W \underline{d}}$$

where B is the between-class scatter matrix, and W is the sum of the within-class scatter matrix.

To solve for the generalized Fisher discriminant directions, take the vector derivative of the above ratio R with respect to \underline{d} and set the resultant equation to zero. The procedure generates the following generalized eigenvector equation.

$$[B - \lambda W]\underline{d} = 0$$
$$[W^{-1}B - \lambda I]\underline{d} = 0$$

The generalized discriminant vectors are the eigenvectors of the nonsymmetric matrix $W^{-1}B$. The rank of the between-class scatter matrix for the K -class discrimination problem is $K - 1$; therefore, no more than $K - 1$ non-zero eigenvector solutions exist. Thus, the generalized discriminant vector function produces $K - 1$ discriminant vectors, with the vectors which correspond to the largest eigenvalues producing the maximum discrimination.

- NLM is accomplished by using the OLPARS routine for multidimensional scaling. This routine iteratively fits the data into a two or three dimensional subspace such that the difference between interpoint distances in the lower and higher dimensional spaces is as small as possible.
- Measurement transformations are arbitrary transformations on the data before any projections are formed. Two "built-in" transformations available are the normalization transformation and the eigenvector transformation. In addition, OLPARS has the capability to perform any arbitrary transformation specified by the user.

2. THE DATA SET

The data set for this study consisted of grid intersection points labeled according to ground-truth class for each of several segments, including 20 segments from the 1976 crop year and 25 segments from the 1977 crop year. For each segment, the grid intersection picture elements (pixels) were sorted by ground-truth class into wheat, barley, rye, oats, flax and other. Each of these classes was further divided into those pixels which were pure and those which were on a boundary. Table 2-1 lists the segments used, their location, and the acquisitions available for each segment.

Not all of the segments in the data set were equally useful. Some contained none or only a small amount of certain small grains. Since rye and flax were not present in large amounts in any segment, it was decided to focus on the separability of spring wheat from barley and oats. Even so, many segments contained only a small amount of one or more of these grains. After an initial exploratory analysis, it was also concluded that boundary pixels had a very detrimental effect on discriminant analysis, eigenvector transformations, and classifier performance. Therefore, border pixels were not used in the study except in cases where very small sample size made their use mandatory.

Figure 2-1 shows a projection on the two largest eigenvectors of the multi-temporal data for segment 1512. Small letters on this figure indicate boundary pixels, and large letters indicate pure pixels. Figure 2-2 shows a Fisher discriminant plane plot for the same data. The results of an identical analysis following removal of boundary pixels are given in figures 2-3 and 2-4. These examples illustrate the effect of boundary pixels in degrading the separability of the pure small-grain pixels.

TABLE 2-1.— SEGMENTS, LOCATION OF SEGMENTS, AND ACQUISITION DATES USED IN THE DATA SET

(a) 1976 crop year segments

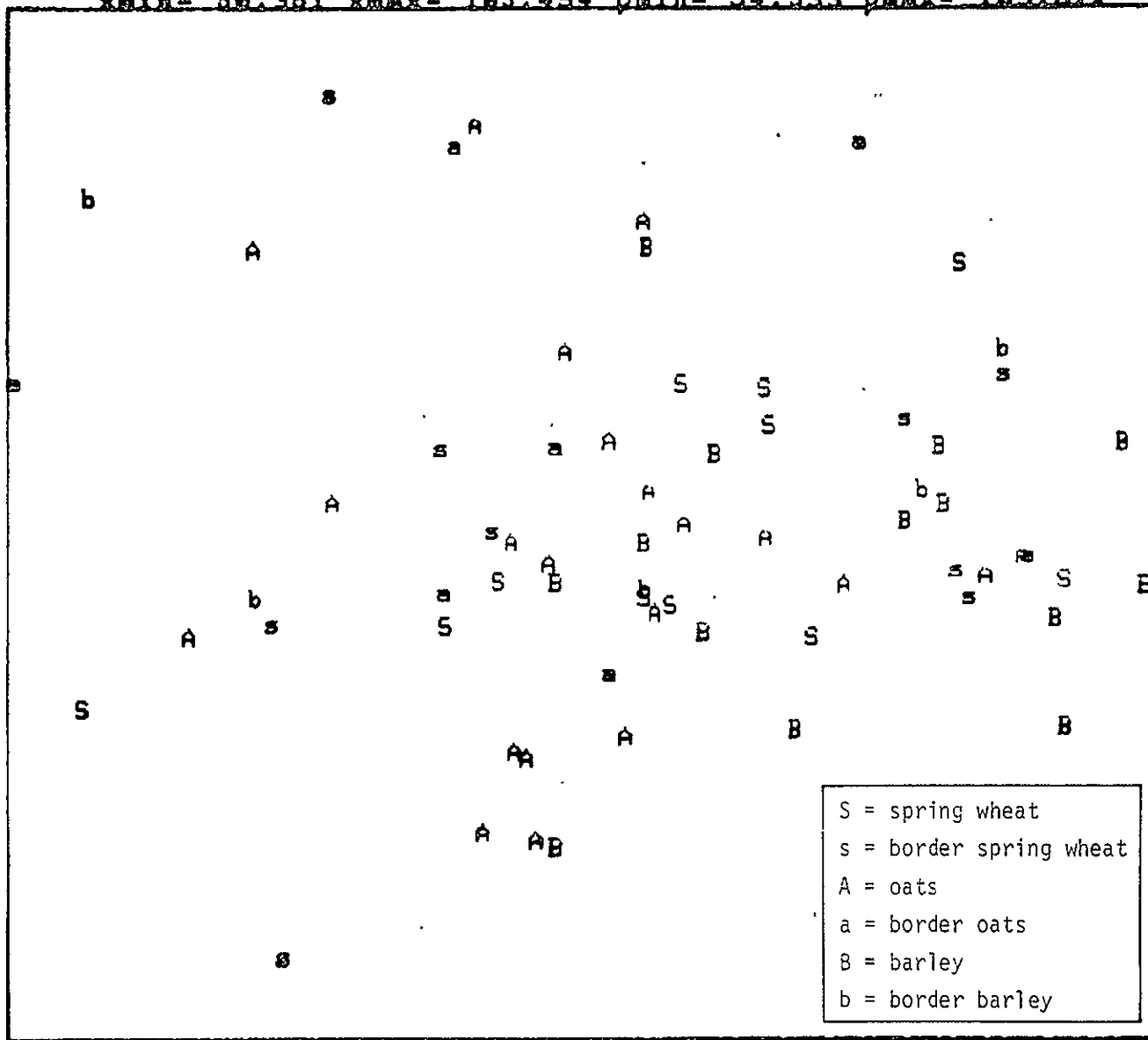
Segment	Location		Acquisitions
	County	State	
1642	Cass	North Dakota	127, 145, 146, 163, 182, 199, 200, 236
1645	Traill	North Dakota	110, 128, 145, 146, 164, 181, 235, 236
1660	Logan	North Dakota	110, 128, 129, 147, 164, 165, 219, 236
1686	Beadle	South Dakota	91, 127, 145, 163, 182, 199, 217
1003	Logan	Colorado	22, 143, 166, 184
1533	Daniels	Montana	116, 152, 187, 205
1559	Wibaux	Montana	150, 204, 240
1614	Pierce	North Dakota	130, 183, 201, 219
1618	Grand Forks	North Dakota	127, 163, 199, 235
1624	Walsh	North Dakota	128, 146, 236, 254
1650	Hettinger	North Dakota	130, 148, 220, 238
1651	Slope	North Dakota	150, 204, 221, 240
1655	Grant	North Dakota	130, 149, 202, 220
1667	Harding	South Dakota	131, 149, 203, 221
1677	Spink	South Dakota	127, 163, 217, 235
1681	Roberts	South Dakota	127, 162, 198, 234
1687	Hand	South Dakota	92, 128, 182, 236
1725	Flathead	Montana	121, 129, 127, 230
1742	Cascade	Montana	(75) 304, 137, 191, 209
1965	Burke	North Dakota	132, 221, 222

TABLE 2-1.— Concluded.

(b) 1977 crop year segments

Segment	Location		Acquisitions
	County	State	
1734	Hill	Montana	95, 113, 203
1747	Judith Basin	Montana	112, 130, 184
1937	Pondera	Montana	132, 168, 203
1663	Richland	North Dakota	120, 121, 138, 139, 156, 157, 174, 175, 193, 211, 229
1667	Harding	South Dakota	71, 107, 125, 143, 161, 179, 197
1648	Bowman	North Dakota	107, 125, 143, 179
1903	Mercer	North Dakota	125, 179, 197, 233
1677	Spink	South Dakota	140, 176, 193, 230
1681	Roberts	South Dakota	120, 139, 175, 192
1512	Clay	Minnesota	120, 156, 157, 193
1513	Kittson	Minnesota	140, 157, 175, 193
1520	Big Stone	Minnesota	120, 156, 174, 192
1523	Wilkin	Minnesota	120, 138, 156, 175
1531	Phillips	Montana	112, 129, 184, 220
1556	Powder River	Montana	162, 180, 198, 235
1725	Flathead	Montana	98, 152, 188, 224
1739	Teton	Montana	114, 150, 168, 222
1742	Cascade	Montana	113, 167, 203
1830	Red Lake	Minnesota	157, 175, 193, 211
1839	Swift	Minnesota	120, 137, 156, 174
1849	Sibley	Minnesota	100, 118, 136, 172
1873	Lincoln	Minnesota	120, 138, 174, 192
1929	Blaine	Montana	112, 147, 184, 220
1930	Hettinger	North Dakota	125, 143, 197, 215
1899	Walsh	North Dakota	122, 157, 175, 193

xmin= 54.351 xmax= 105.494 ymin= 54.533 ymax= 109.677



drawbody
 redraw
 restruct
 eliacles
 index
 seq
 dboundary
 scaleszm
 scalesrt
 cdisplay
 cprint
 ver\$save

S = spring wheat
 s = border spring wheat
 A = oats
 a = border oats
 B = barley
 b = border barley

Current
 Option:
 eigv\$aa2

Dataset:
 77tr1512
 ### x 1728

ORIGINAL PAGE IS
 OF POOR QUALITY

2-4

projected on meas. 1 and 2 scatter plot

Figure 2-1.— Eigenvector projection with boundary pixels, segment 1512.

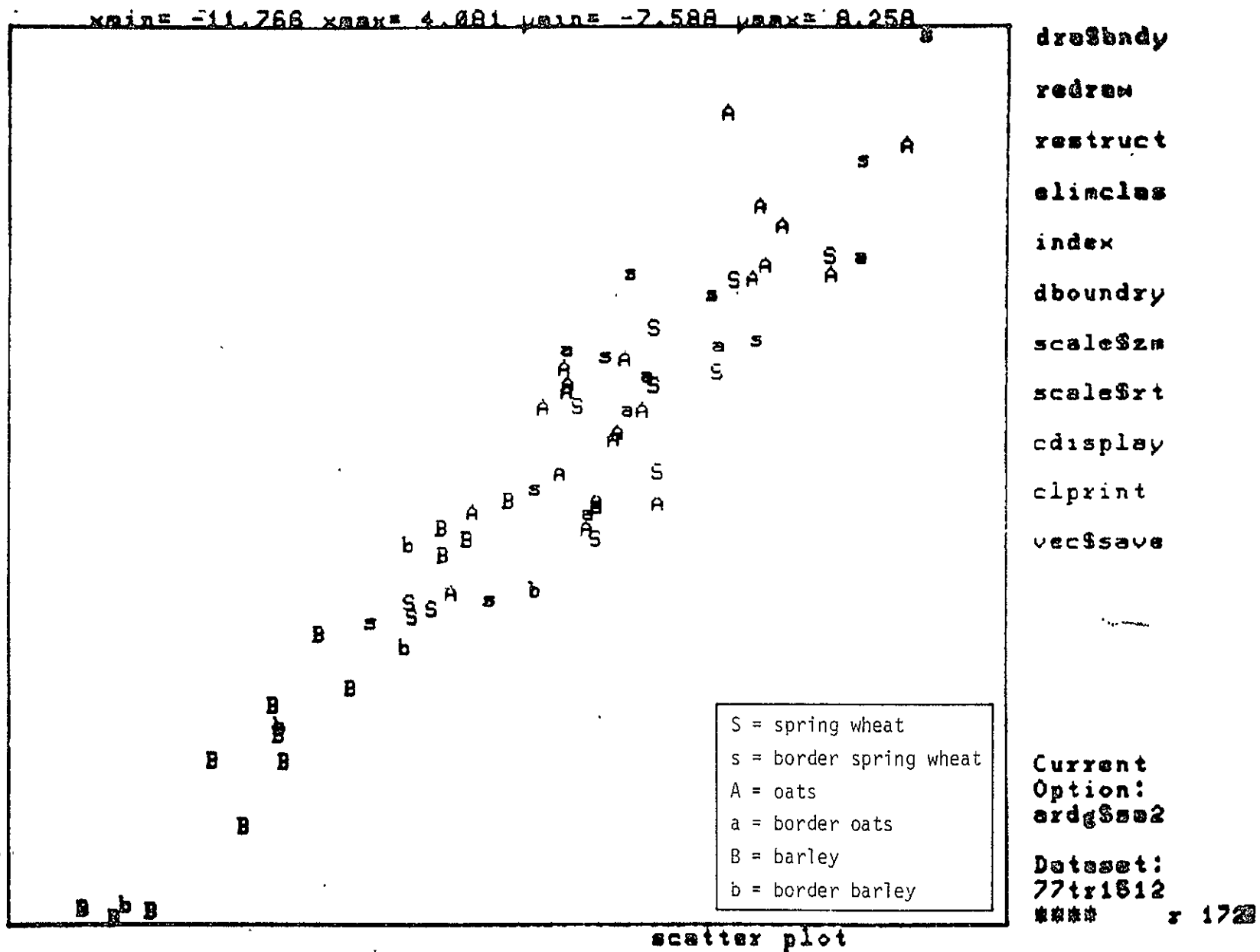
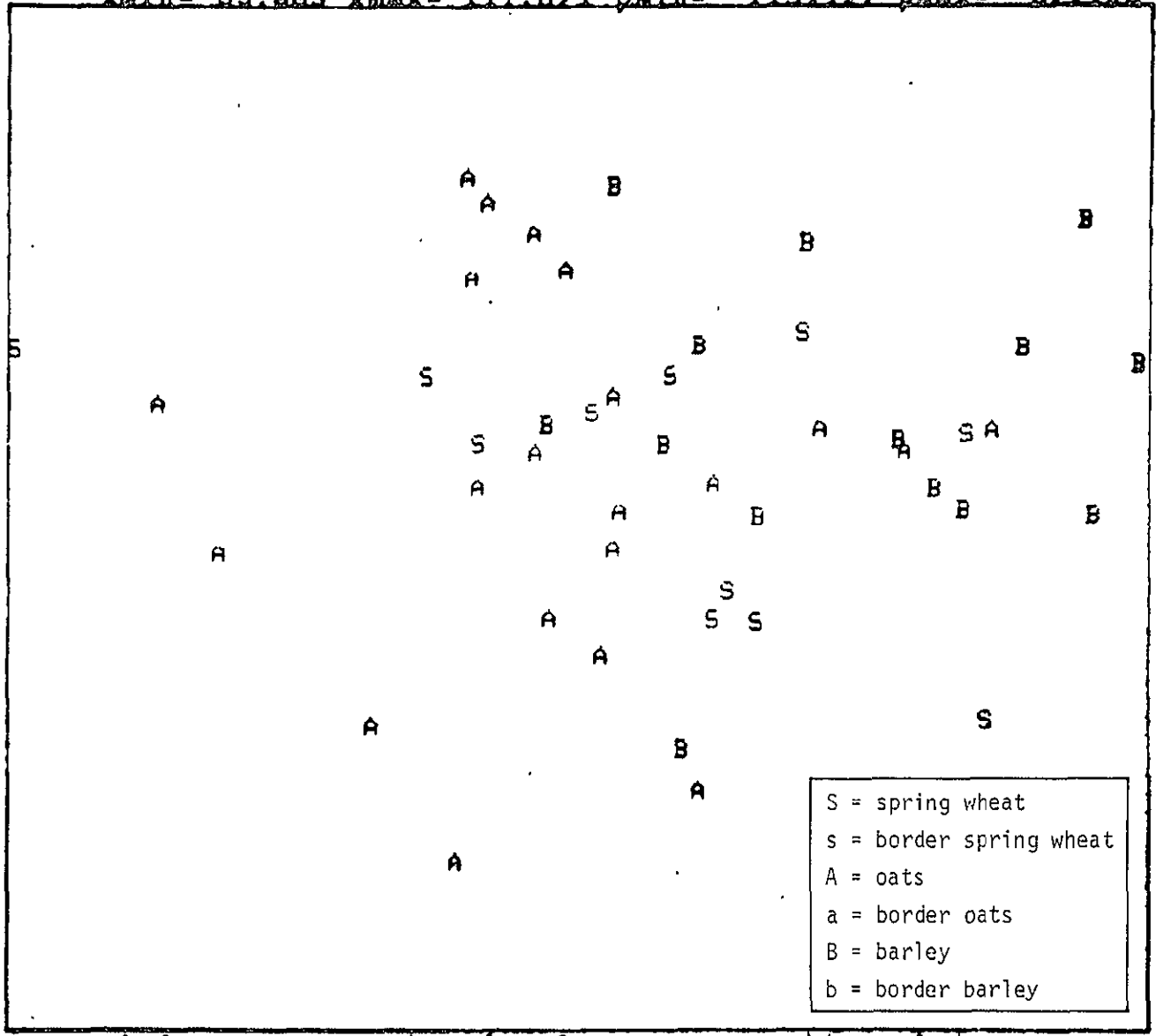


Figure 2-2.— Fisher discriminant vector projection with boundary pixels, segment 1512.

xmin= 55.869 xmax= 111.871 ymin= -113.127 ymax= -57.125



drawbody
 redren
 restruct
 slicles
 index
 seq
 dboundary
 scaleszm
 scalesxt
 cdisplay
 clprint
 veesave

ORIGINAL PAGE IS
OF POOR QUALITY

S = spring wheat
 s = border spring wheat
 A = oats
 a = border oats
 B = barley
 b = border barley

Current
 Option:
 sigv\$se2
 Dataset:
 77tr1512

x 170

projected on axes. 1 and 2 scatter plot

Figure 2-3.— Eigenvector projection without boundary pixels, segment 1512.

2-6

12

2-7

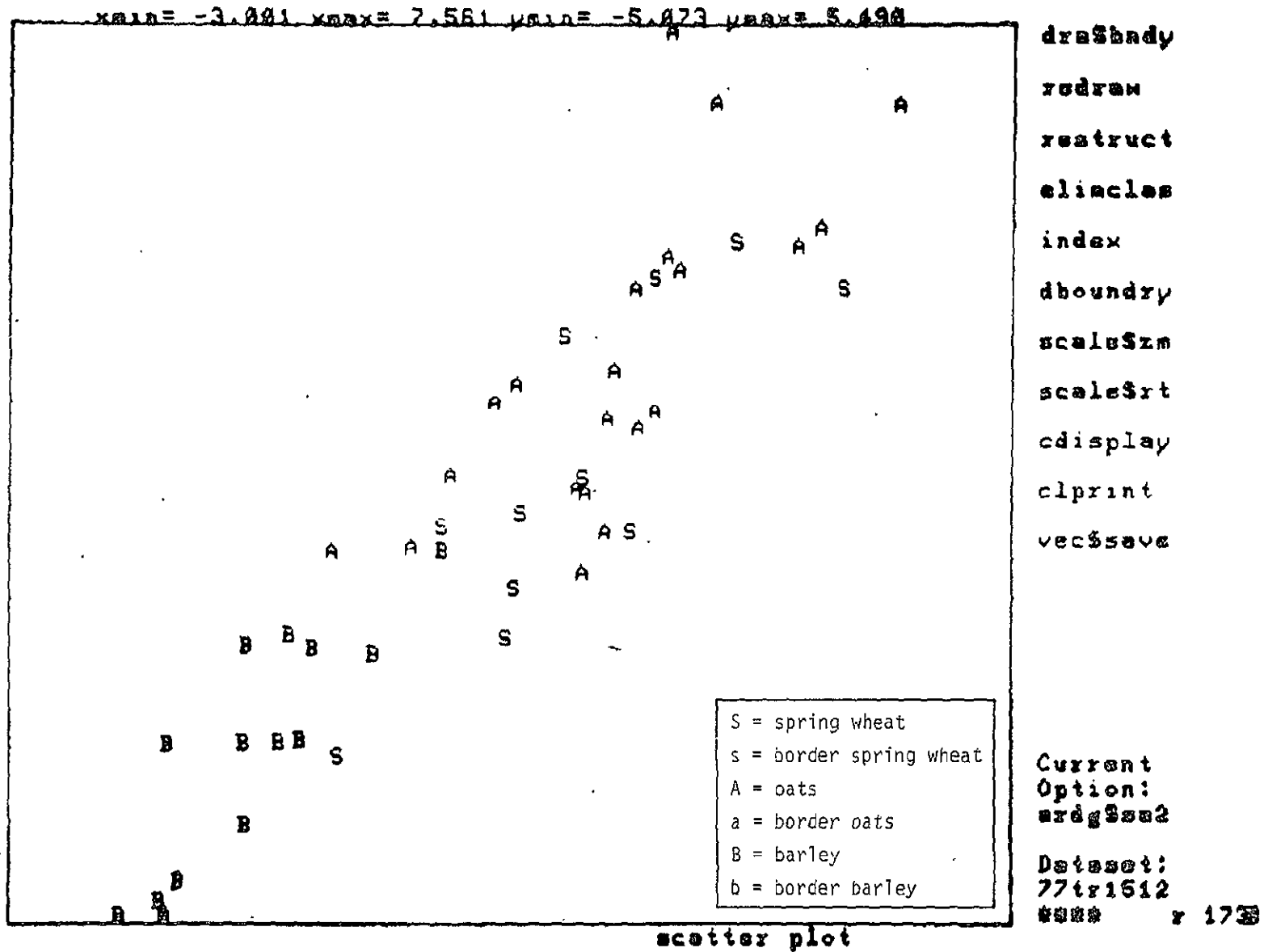


Figure 2-4.— Fisher discriminant vector projection without boundary pixels, segment 1512.

3. SEPARABILITY ANALYSIS OF WHEAT AND OTHER SMALL GRAINS

3.1 SEPARABILITY AS A FUNCTION OF CROP CALENDAR

In order to assess the spectral separability of wheat from other small grains as a function of crop calendar, two approaches were taken. First, each acquisition for a segment was examined in the Fisher discriminant plane and also in the plane associated with the first two eigenvectors of the pooled covariance matrix for each class. These projections are described in section 1.2. And second, after a visual inspection and comparison of the various acquisitions in these two dimensional subspaces, each acquisition was classified using the NMV classifier and the Fisher pairwise classifier. These classifiers were trained using all of the data for each segment and were then applied to the training data. The probability of correct classification (PCC) resulting from these classifications provides numerical measures of the separability of spring wheat from other small grains.

Figures 3-1 through 3-4 show the sequence of eigenvector projections for segment 1830 (77) corresponding to acquisition dates of 157 (77), 175 (77), 193 (77), and 211 (77). Figures 3-5 through 3-8 show the corresponding Fisher discriminant plane projections. This segment was chosen for inclusion in the report because it is representative of trends observed over many segments. These trends may be summarized as follows:

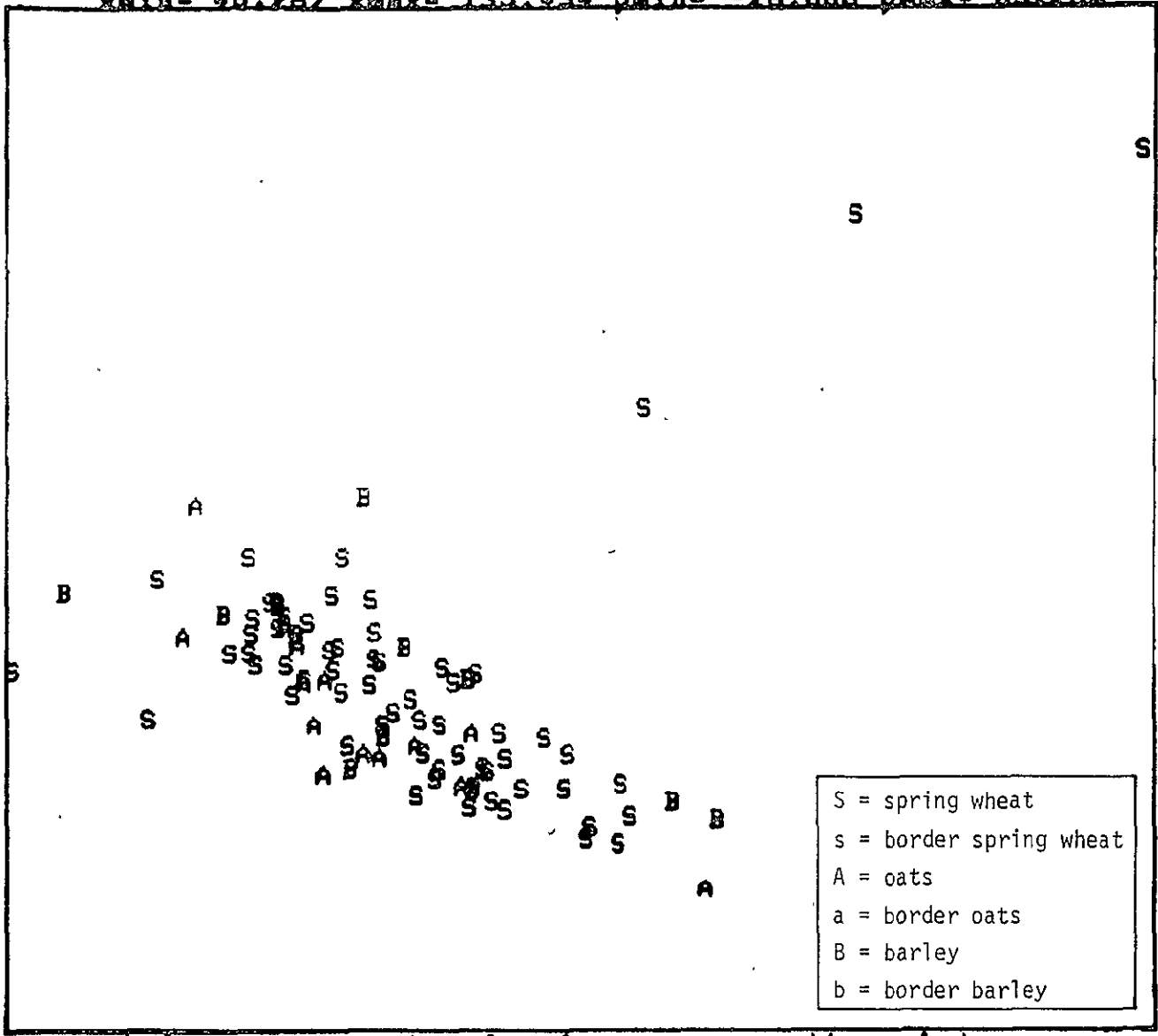
- a. On a single-acquisition basis, barley is not separable from wheat except at a certain critical time in the growing season which corresponds to a Robertson biostage for wheat of approximately 5.0 to 5.9. It appears that this separation occurs because barley turns color from green to yellow earlier than wheat.
- b. On a single-acquisition basis, oats are not significantly separable from wheat at any time during the growing season.

Table 3-1 gives the PCC estimates calculated using NMV classification for several of the 1977 crop year segments which contained significant amounts

TABLE 3-1.- THE PCC FOR SPRING WHEAT

Segment	Robertson biostage for spring wheat					
	0 to 1.9	2.0 to 2.9	3.0 to 3.9	4.0 to 4.9	5.0 to 5.9	6.0 to 7.0
1512	36.4	36.4			63.6	
1830			53.9	67.7	58.5	40.0
1899	50.0		46.3	64.8	81.5	
1648		79.3	79.3	89.7		
1742	30.0		90.0			80.0
1929	87.9		48.5		81.8	78.8
1681	57.1	71.4		67.9		42.9
1523	48.3	37.9	37.9	75.9		
Average	51.6	56.3	59.3	73.2	71.4	60.4
Overall average						62.0

xmin= 45.287 xmax= 135.434 ymin= -26.886 ymax= 63.268



dra\$bdy
redren
restruct
elincles
index
seq
dboundary
scale\$zn
scale\$rt
cdisplay
clprint
vec\$ave

Current
Option:
sig\$ss2

Dataset:
157t1830

r 170

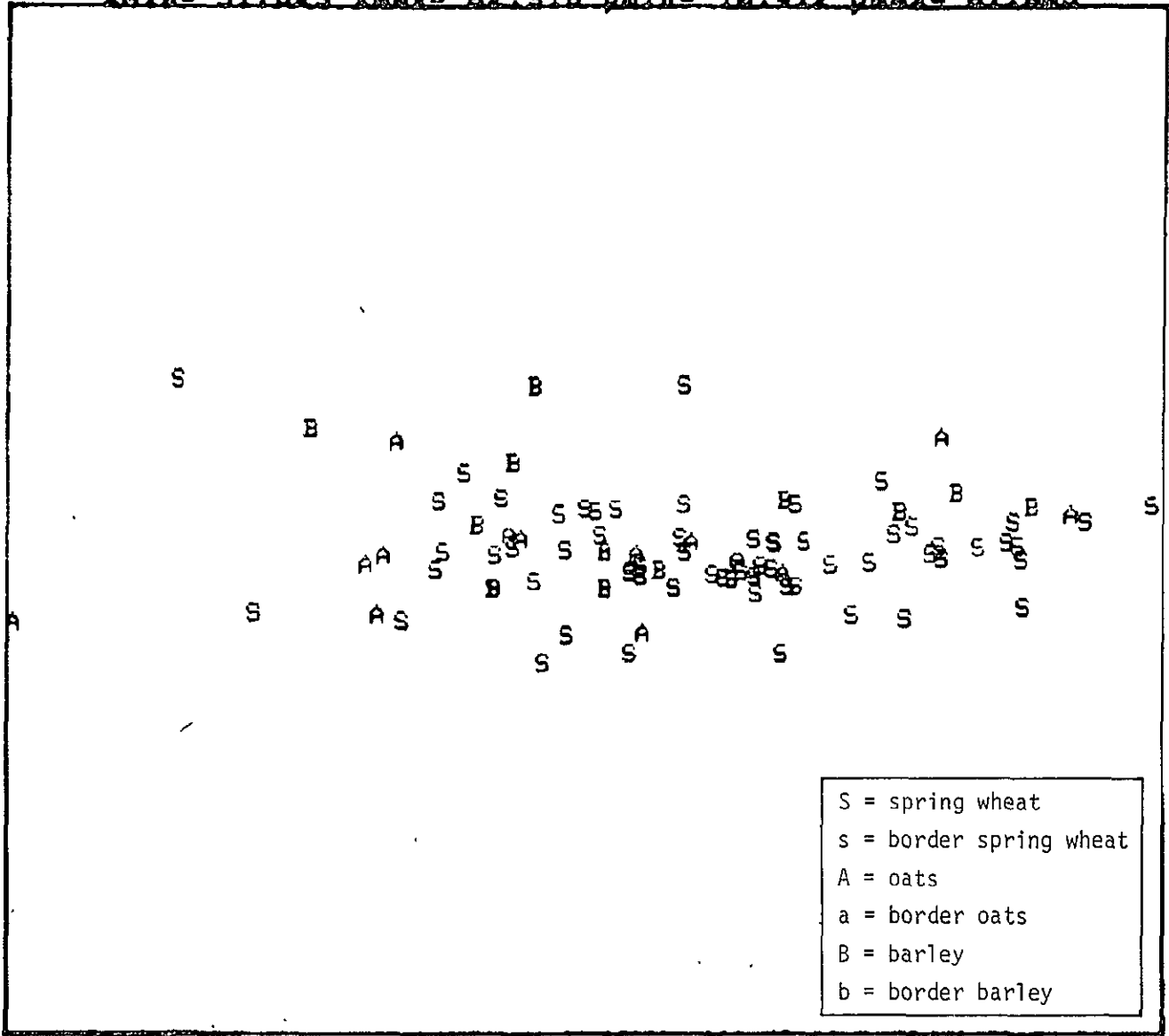
ORIGINAL PAGE IS
OF POOR QUALITY

3-3

16

Figure 3-1.— Eigenvector projection, segment 1830, day 157.

xmin= 31.523 xmax= 82.916 ymin= 10.412 ymax= 61.005



S = spring wheat
 s = border spring wheat
 A = oats
 a = border oats
 B = barley
 b = border barley

dre\$bdy
 redraw
 restruct
 elincls
 index
 seq
 dboundry
 scale\$za
 scale\$rt
 cdisplay
 clprint
 vec\$save

Current
 Option:
 eigv\$se2
 Dataset:
 175t1030
 ##### r 170

projected on axes. 1 and 2 scatter plot

Figure 3-2.- Eigenvector projection, segment 1830, day 175.

3-4

11

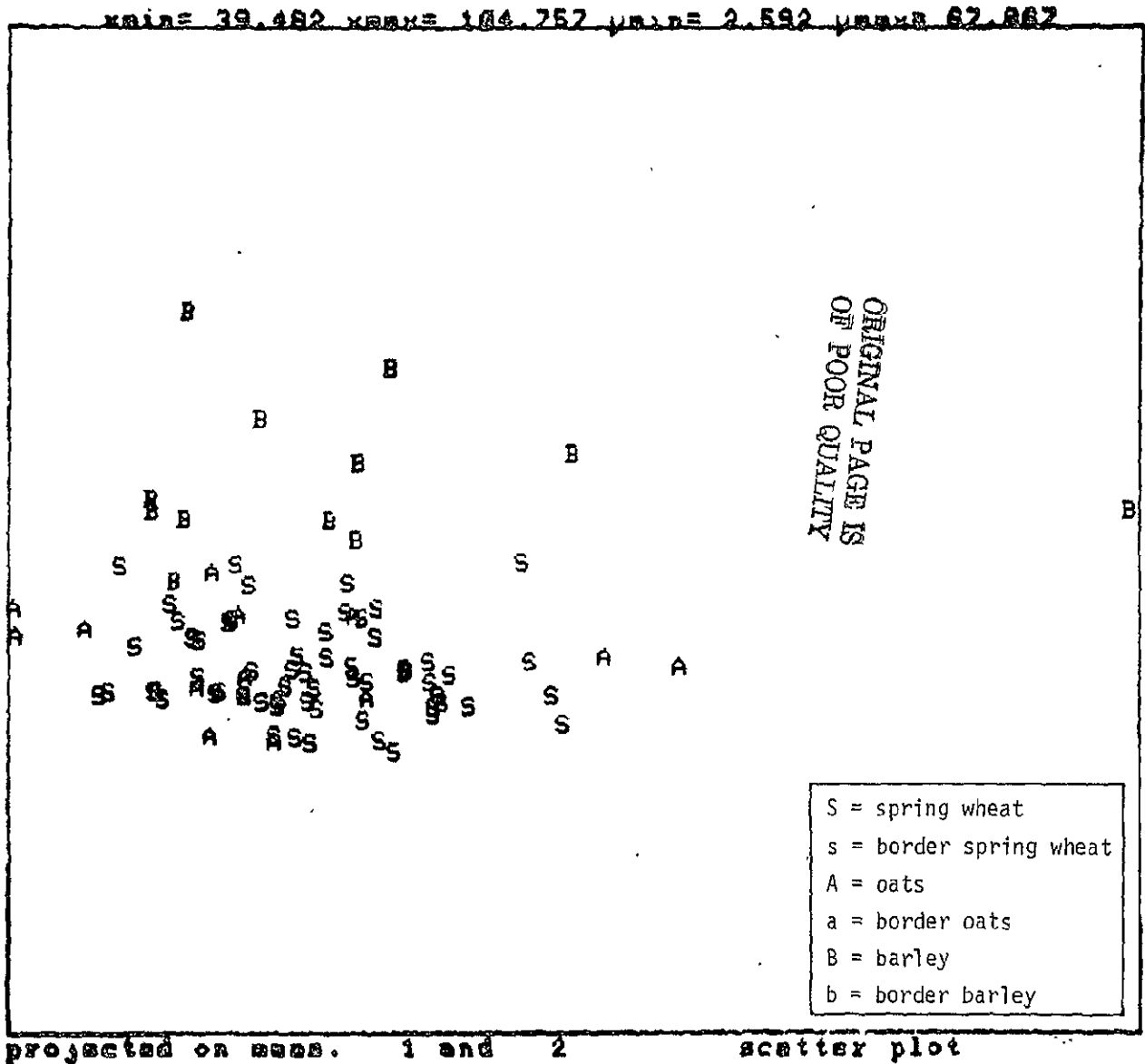
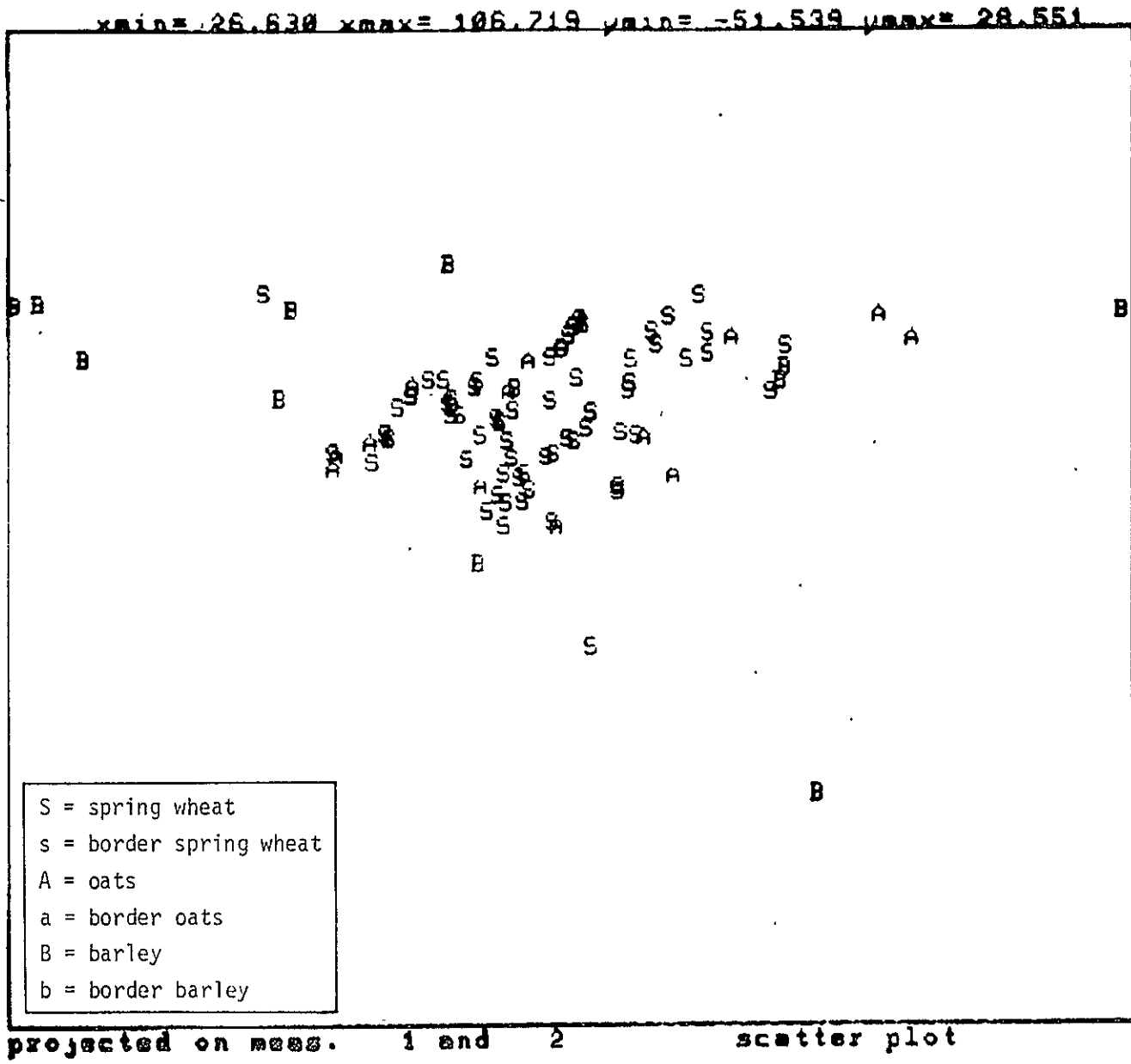


Figure 3-3.— Eigenvector projection, segment 1830, day 193.

3-5



```

drawbody
redraw
restruct
elinclab
index
seq
dboundary
scale$zm
scale$rt
cdisplay
clprint
vec$save

```

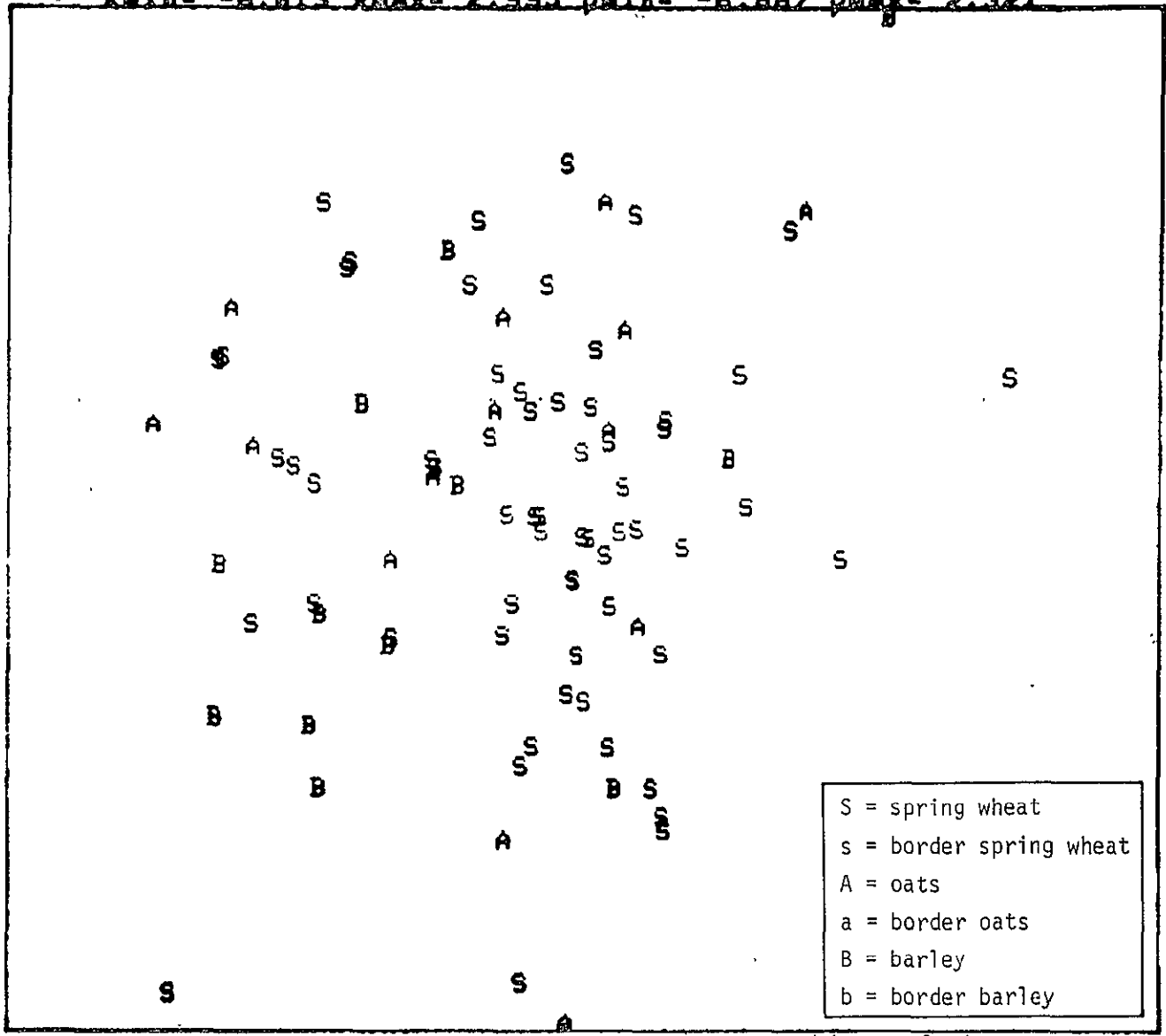
```

Current
Option:
eigv$se2
Dataset:
211t1030
**** r 100

```

Figure 3-4.— Eigenvector projection, segment 1830, day 211.

xmin = -6.013 xmax = 2.995 ymin = -6.687 ymax = 2.321



S = spring wheat
 s = border spring wheat
 A = oats
 a = border oats
 B = barley
 b = border barley

drawbody
 readran
 restruct
 elincls
 index
 dboundary
 scalesa
 scalesrt
 cdisplay
 clprint
 vcsave

Current
 Option:
 ord 6 6 2
 Dataset:
 157t1830

r 17

ORIGINAL PAGE IS
 OF POOR QUALITY

scatter plot

Figure 3-5.— Fisher discriminant projection, segment 1830, day 157.

3-7

20

3-8

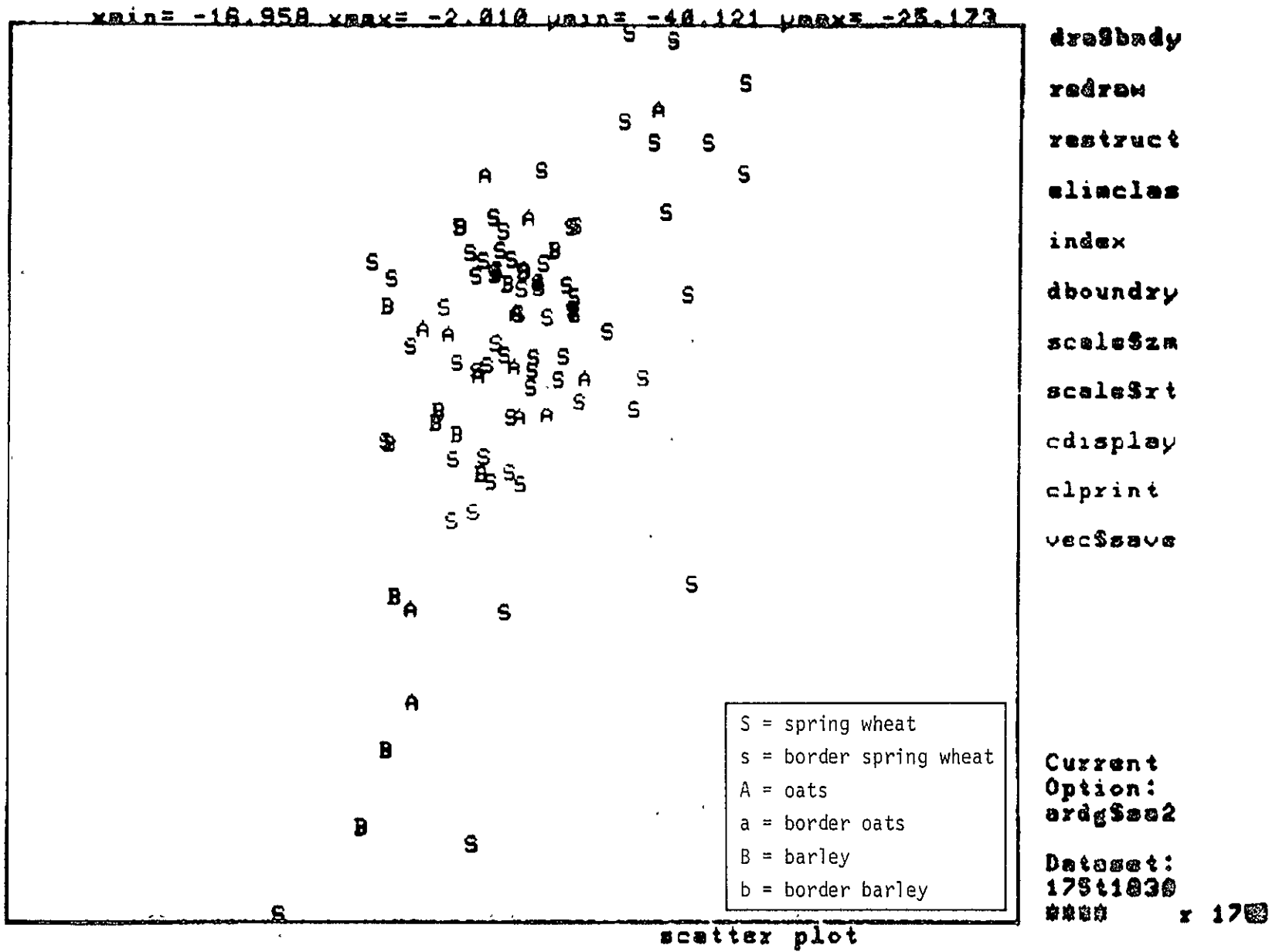
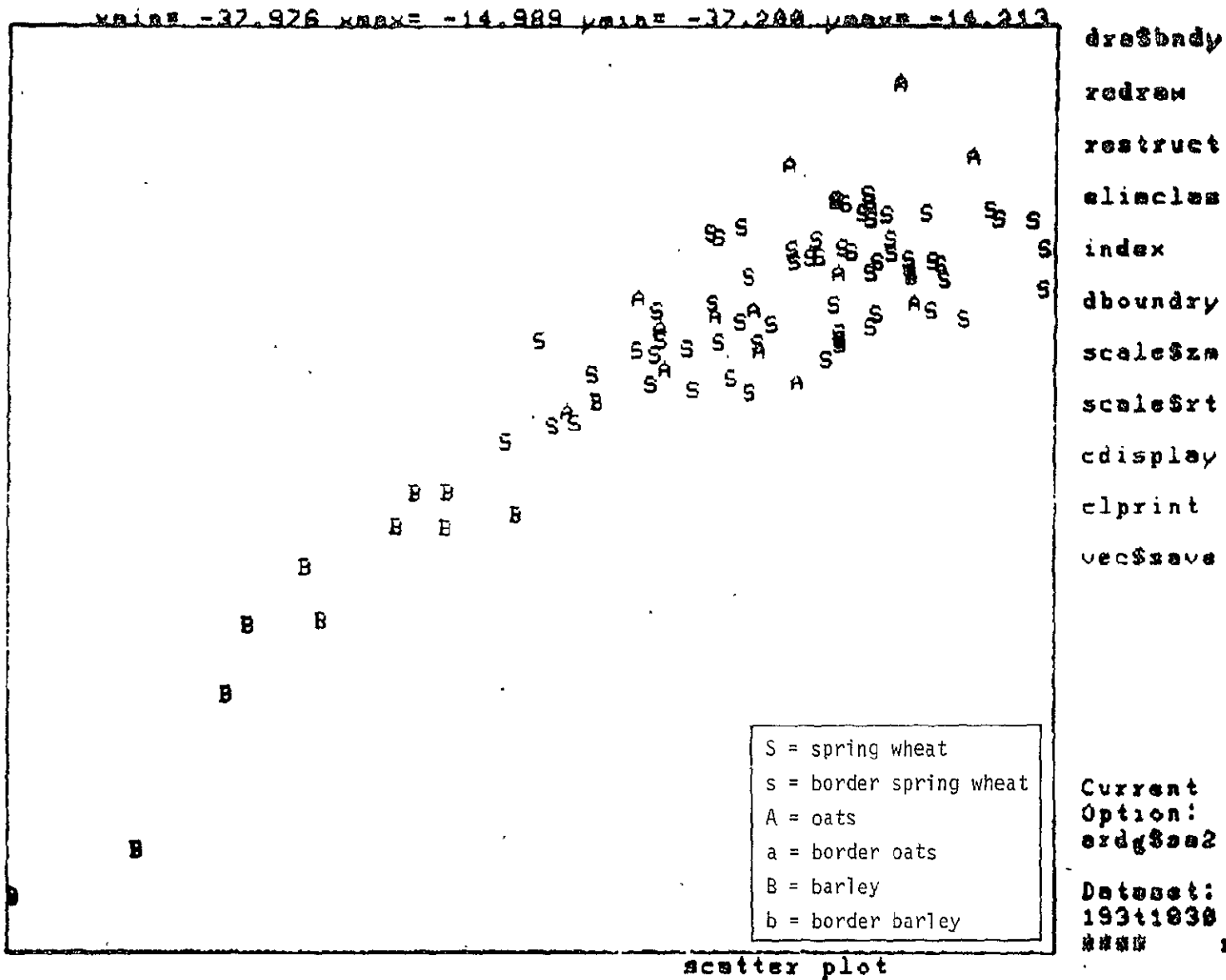


Figure 3-6.— Fisher discriminant projection, segment 1830, day 175.

21



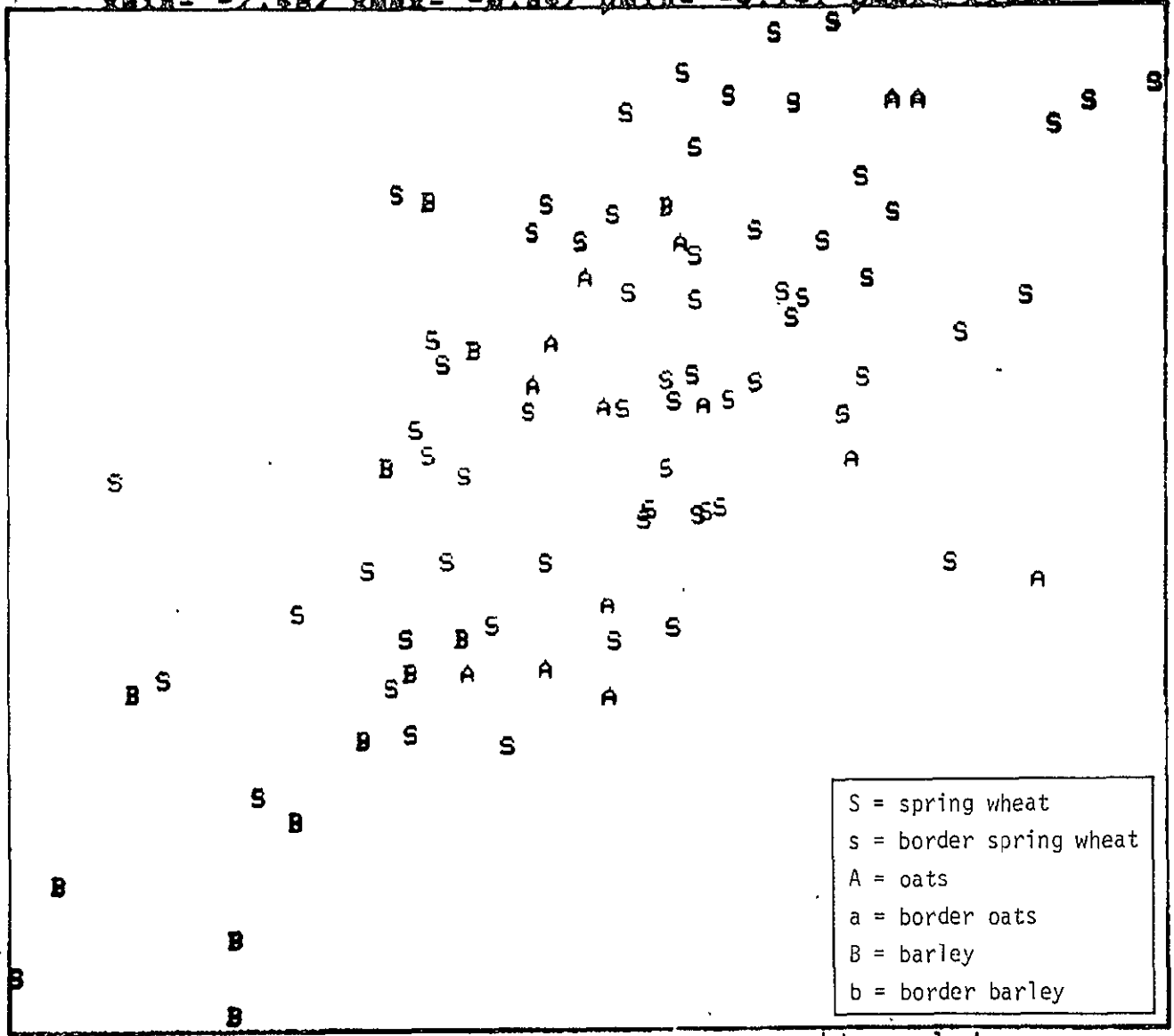
ORIGINAL PAGE IS
OF POOR QUALITY

Current
Option:
ordg\$aa2

Dataset:
193+1830
r 100

Figure 3-7.— Fisher discriminant projection, segment 1830, day 193.

xmin = -7.487 xmax = -0.847 ymin = -4.141 ymax = 2.499



dya@bndy
 redren
 restruct
 eliacles
 index
 dboundary
 scale\$za
 scale\$xt
 cdisplay
 clprint
 vec\$zave

Current
 Option:
 ordg\$z2

Dataset:
 211+1830
 **** x 1013

scatter plot

Figure 3-8.— Fisher discriminant projection, segment 1830, day 211.

3-10

23

of spring wheat and either barley or oats. The PCC values reported in table 3-1 are computed by taking the proportion of the spring wheat pixels which were correctly classified for each acquisition of each segment. The acquisitions have been grouped to correspond to Robertson biostage ranges for spring wheat. Average PCC values are shown for each Robertson biostage range. These results demonstrate that the maximum separability of spring wheat from barley and oats occurs during Robertson biostage 4.0 to 5.9 for spring wheat. The separability at other growth stages is quite poor.

Tables 3-2 and 3-3 give the corresponding PCC estimates for the class of barley pixels and the class of oats pixels for each segment, respectively. The average PCC values show that the best separation of barley from spring wheat and oats occurs during Robertson biostage 5.0 to 7.0 for spring wheat. This overlaps with the period during which spring wheat showed the best separability, the overlap being from Robertson biostage 5.0 to 5.9 for spring wheat.

Oats showed some separability from barley and spring wheat during Robertson spring wheat biostages 0 to 1.9 and 5.0 to 5.9.

These observations drawn from the classification results confirm the analysis made using Fisher and eigenvector projections. In the light of both analyses, it is clear that an acquisition during Robertson biostage 5.0 to 5.9 for spring wheat provides the best unitemporal separability of spring wheat, oats, and barley. Visual analysis of the projected data revealed that barley was typically separable from spring wheat and oats at this time; however, using only a single acquisition, oats were not significantly separable from spring wheat at this time, or any other time during the growing season.

3.2 MULTITEMPORAL SEPARABILITY

In order to investigate the multitemporal separability of wheat from other small grains, projections of multitemporal data into the Fisher discriminant plane and the plane associated with the two largest eigenvectors of the pooled covariance matrix were visually examined. It was found that multitemporal

TABLE 3-2.- THE PCC FOR BARLEY

Segment	Robertson biostage for spring wheat					
	0 to 1.9	2.0 to 2.9	3.0 to 3.9	4.0 to 4.9	5.0 to 5.9	6.0 to 7.0
1512	28.6	64.3			78.6	
1830			66.7	66.7	31.7	100.0
1899	67.7		88.7	75.8	90.3	
1648		50.0	50.0	50.0		
1742	92.3		84.6			100.0
1929	54.6		63.6		90.9	81.8
1681	14.3	14.3		71.4		71.4
1523	72.2	61.6	88.9	55.6		
Average	55.0	47.6	73.8	63.9	87.9	88.3
Overall average						69.4

TABLE 3-3.- THE PCC FOR OATS

Segment	Robertson biostage for spring wheat					
	0 to 1.9	2.0 to 2.9	3.0 to 3.9	4.0 to 4.9	5.0 to 5.9	6.0 to 7.0
1512	95.2	57.1			71.4	
1830			64.3	50.0	71.4	50.0
1899						
1648		83.3	50.0	33.3		
1742						
1929						
1681	85.7	81.0		66.7		81.0
1563	46.7	46.7	60.0	53.3		
Average	75.9	67.0	58.1	50.8	71.4	65.5
Overall average						64.8

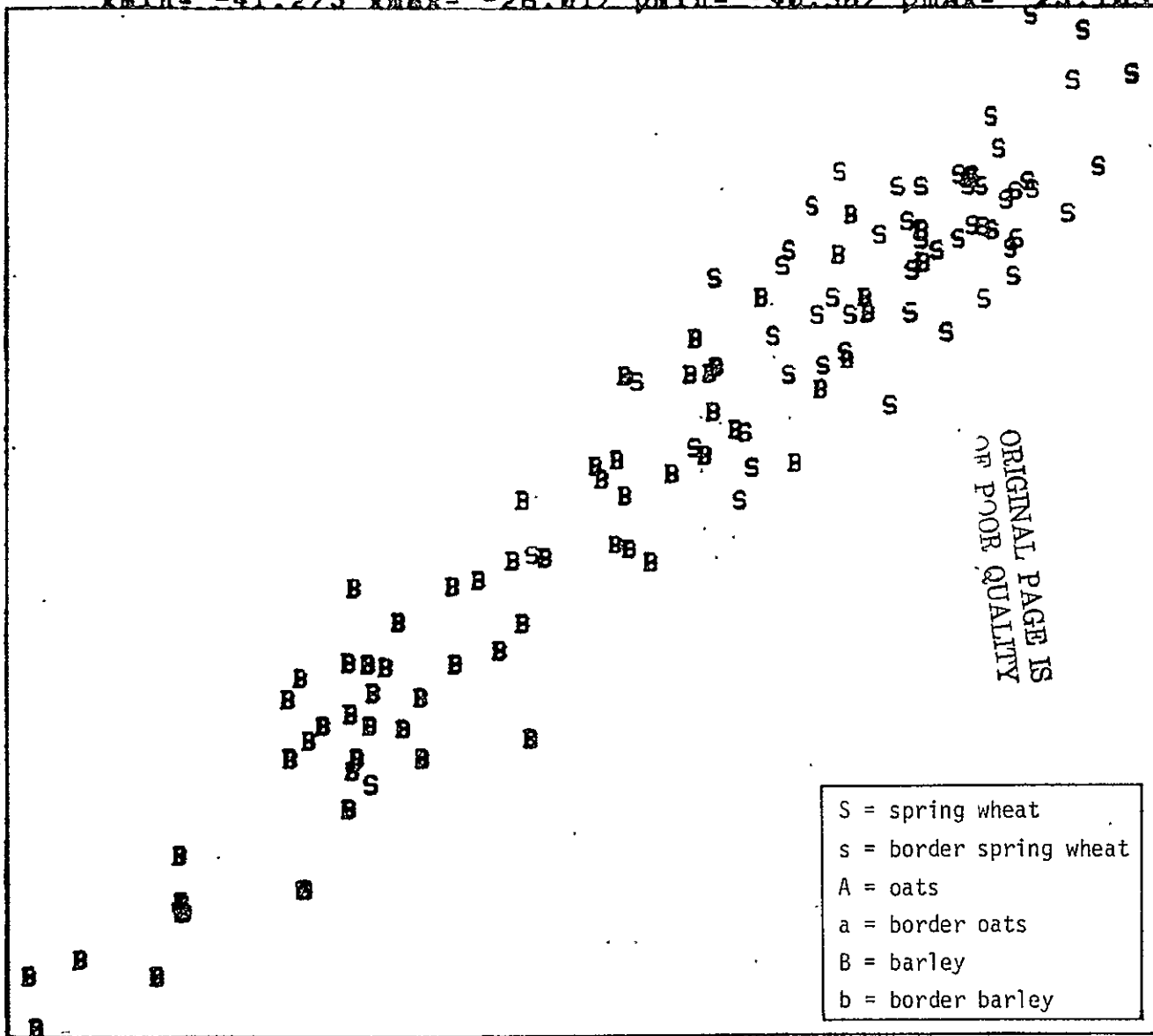
separability was better than that which would be obtained on any single date. Other segment results were as follow:

- a. If a single acquisition around the turning time for barley is available, it generally contains most of the multitemporal spring wheat and barley separability.
- b. If a single acquisition around the turning time for barley is not available, there is still significant multitemporal spring wheat and barley separability.
- c. Occassionally, oats show multitemporal separability from spring wheat and barley.

Figures 3-9 and 3-10 show the Fisher discriminant plane projections for segment 1899 (77). Figure 3-9 shows a projection of multitemporal data including acquisition dates 122 (77), 157 (77), 175 (77), and 193 (77), while figure 3-10 shows a projection for unitemporal data from acquisition 193 (77). The overall PCC values for NMV classification of these same two groups of data are 93.1 percent for the multitemporal data and 86.2 percent for the unitemporal data. Thus, most of the spring wheat and barley separability is contained in the single acquisition. This result is typical for those segments containing an acquisition near the critical time for barley.

Figure 3-11 shows a Fisher discriminant plane projection for multitemporal data from segment 1929. These data consist of acquisitions 112 (77), 147 (77), 184 (77), and 220 (77). Although none of these acquisitions correspond to the turning time for barley, there is evident separability, and the PCC for NMV classification of these data is 100 percent. Figure 3-12 shows the Fisher projection for day 184, which was the best of the four unitemporal projections. The separation is obviously very poor, and the overall PCC from NMV classification of this unitemporal data is 84 percent.

xmin = -41.275 xmax = -26.017 ymin = -40.367 ymax = -25.109



scatter plot

```

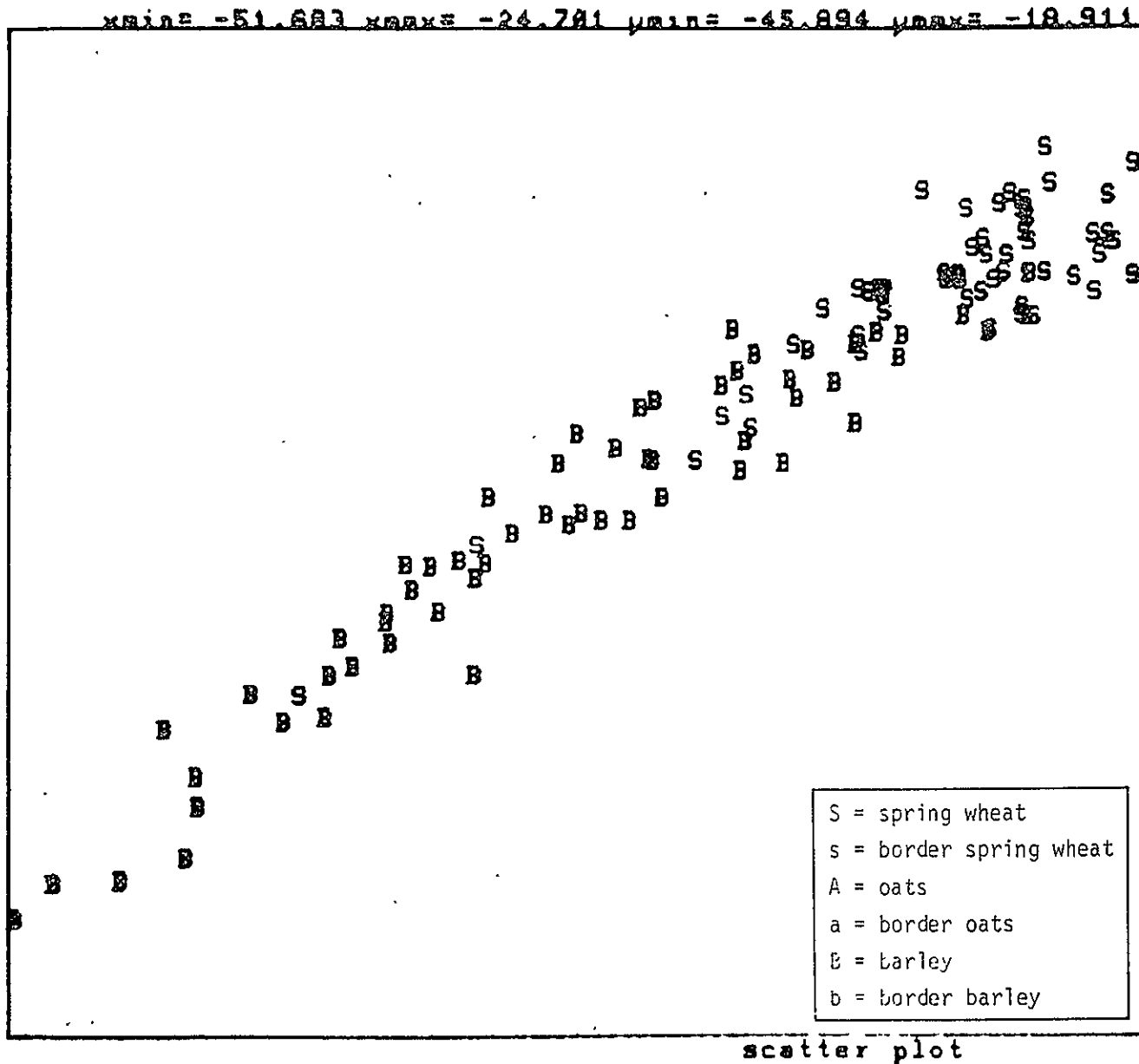
dres$bdy
redraw
restruct
elimclass
index
dboundary
scale$zm
scale$rt
cdisplay
clprint
vec$save

```

Current Option:
erdg\$as2

Dataset:
77tr1899
x 172

Figure 3-9.— Multitemporal Fisher discriminant vector projection, segment 1899.



```

dresbody
redres
restruct
eliasles
index
dboundary
scale$zw
scale$rt
cdisplay
clprint
vecsave

```

ORIGINAL PAGE IS
OF POOR QUALITY

```

Current
Option:
ord$S22

```

```

Dataset:
193T1899
****

```

r 173

scatter plot

Figure 3-10.-- Fisher discriminant vector projection, segment 1899, day 193.

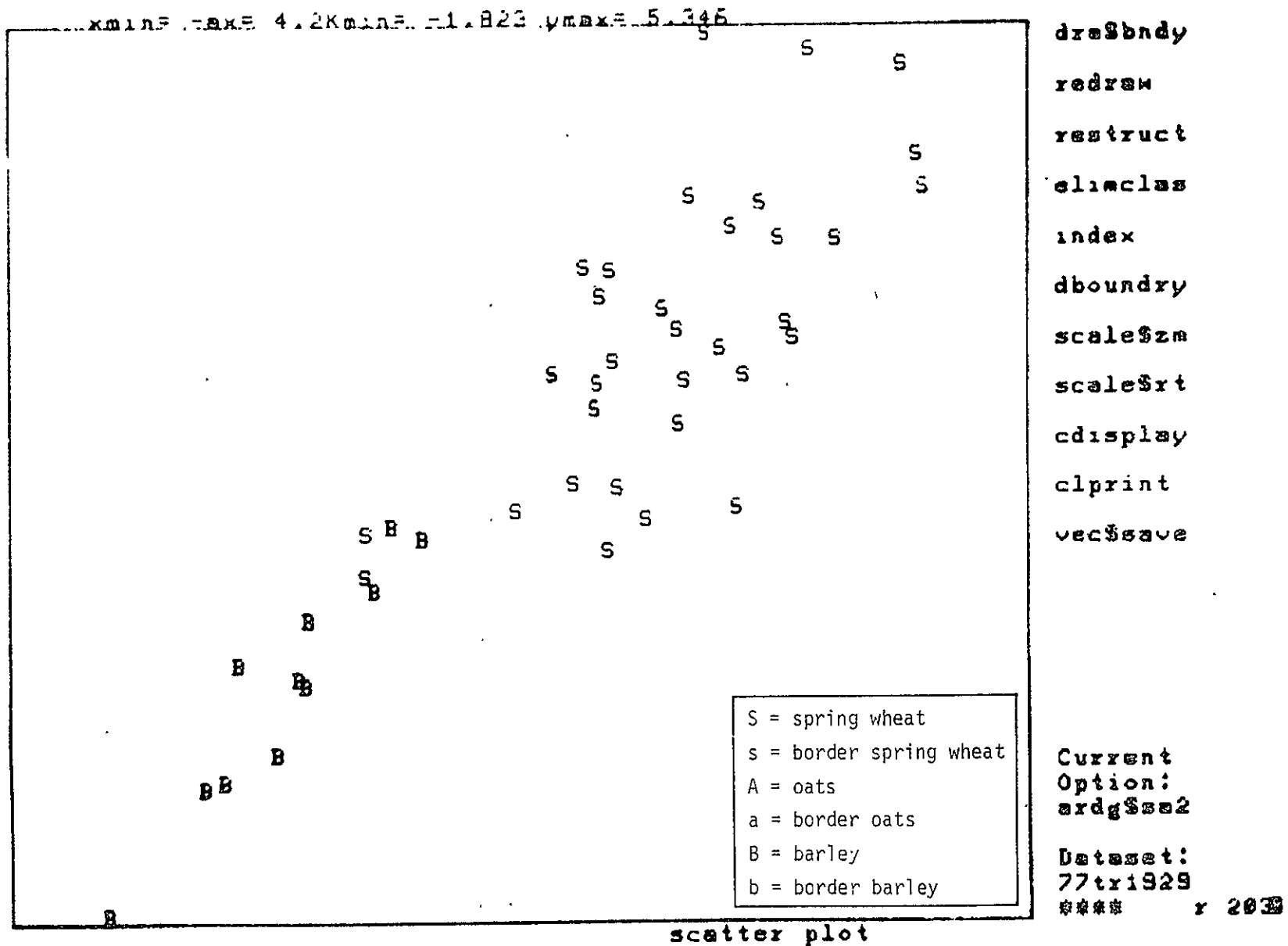
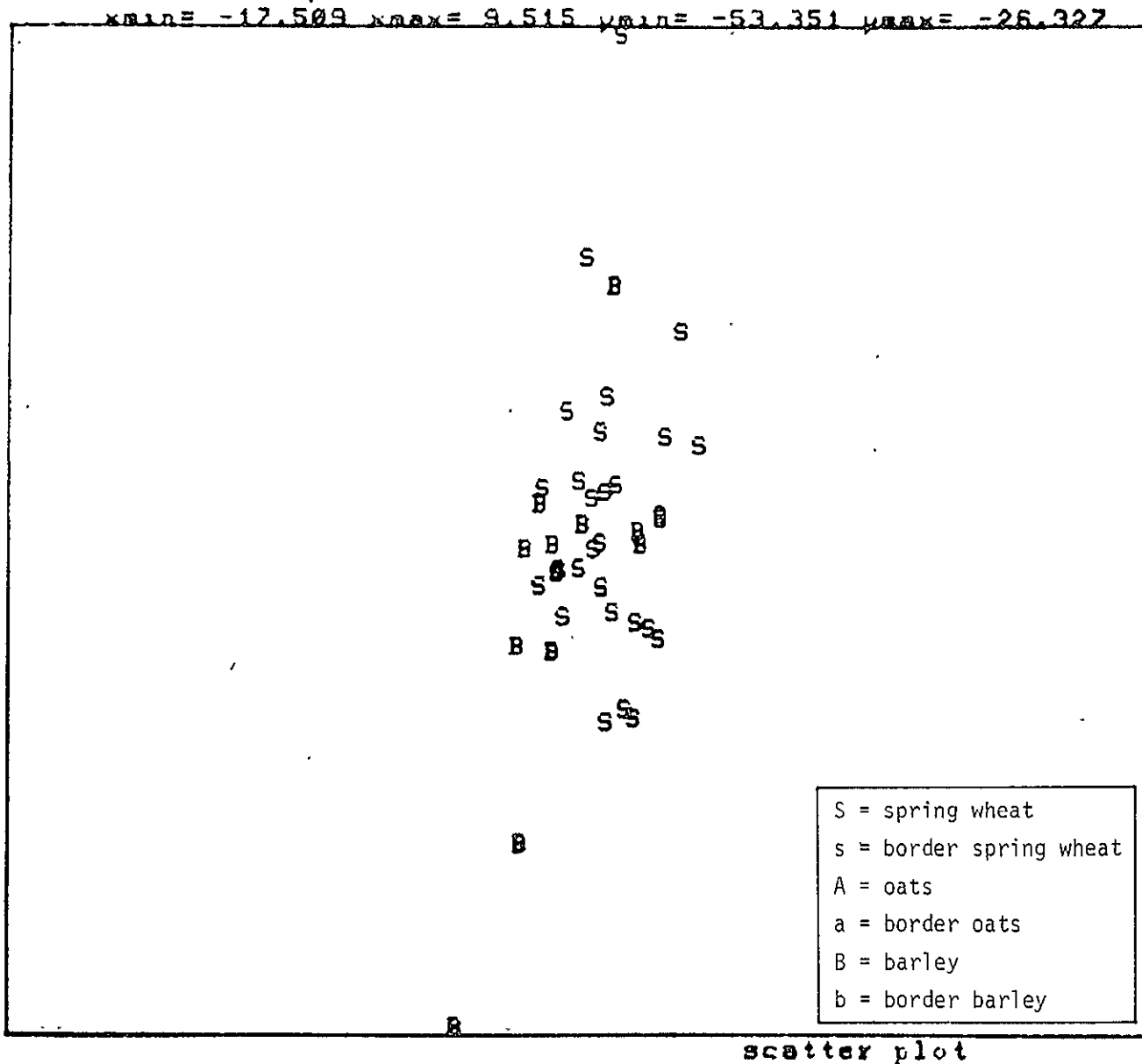


Figure 3-11.— Multitemporal Fisher discriminant vector projection, segment 1929.



```

dresbndy
redraw
restruct
elinclae
index
dboundary
scale$zm
scale$xt
cdisplay
clprint
vec$save

```

ORIGINAL PAGE IS
OF POOR QUALITY

```

Current
Option:
ordg$se2

```

```

Dataset:
104-T1929
**** r 20

```

Figure 3-12.— Fisher discriminant vector projection, segment 1929, day 184.

Figure 3-13 shows a generalized Fisher discriminant plane projection for multi-temporal data from segment 1681. There are samples from barley, oats, and spring wheat in this segment; the acquisition dates are 127 (77), 162 (77), 198 (77), and 234 (77). Clearly, there is significant multitemporal separability of all three classes in this case. Unfortunately, such separability was not observed frequently enough in the data set to arrive at any conclusions as to its origin.

Table 3-4 gives the list of PCC estimates for the spring wheat, oats, and barley classes using the same segments which appear in tables 3-1, 3-2, and 3-3. By comparing table 3-4 with these previous tables, the conclusions (a) and (b), stated previously, may be verified.

TABLE 3-4.- MULTITEMPORAL PCC'S BY CROP CLASS

Segment	Spring wheat	Barley	Oats	Overall
1512	100.00	92.9	90.5	93.9
1830	100.00	100.00		100.0
1899	87.0	98.4		93.1
^a 1648	100.0	100.0		100.0
1742	100.0	100.0		100.0
^a 1929	100.0	100.0		100.0
1681	78.6	100.0	76.2	80.4
^a 1523	100.0	94.4	93.3	96.8

^aDo not have an acquisition in Robertson biostage 5.0 to 6.0.

3-19

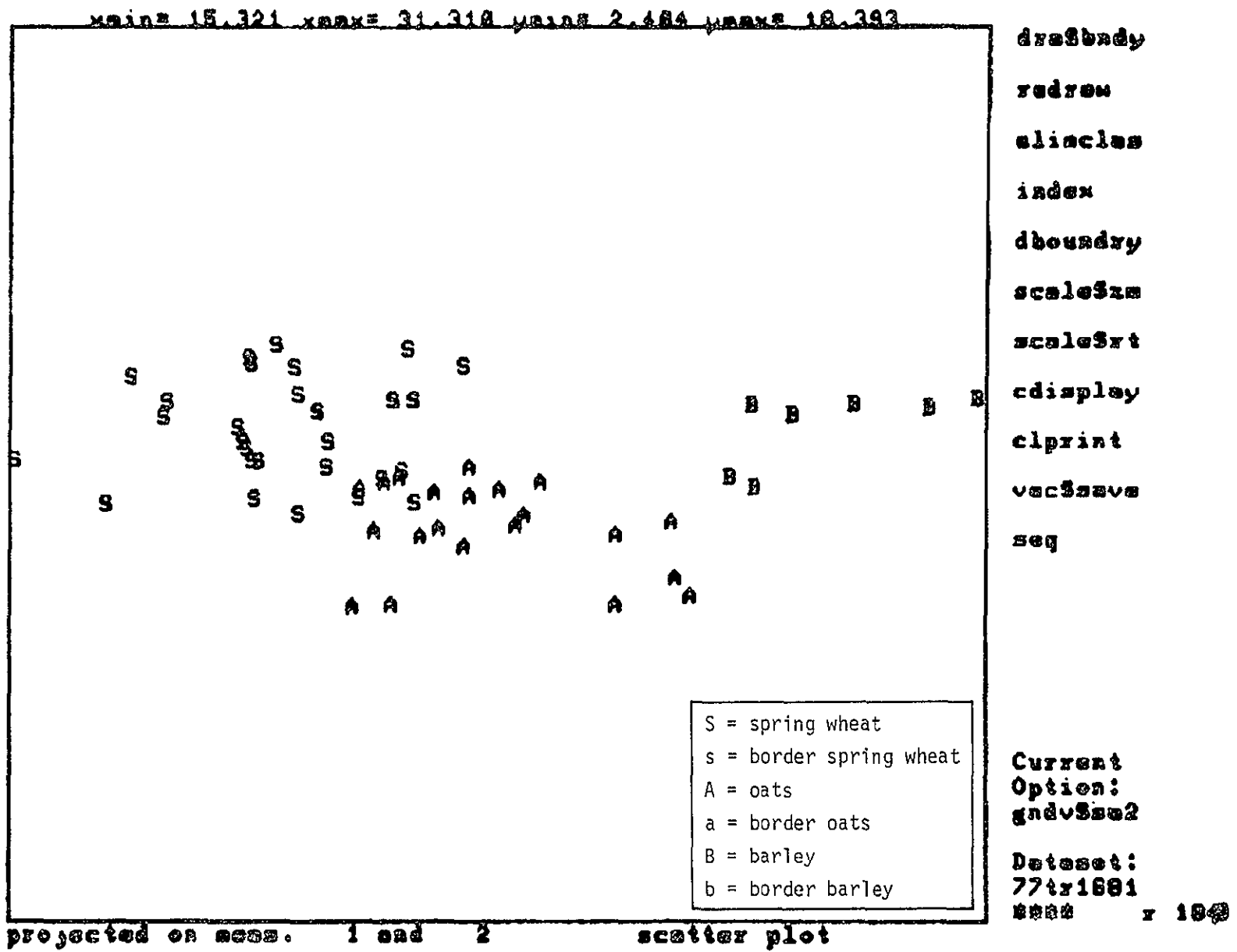


Figure 3-13.— Multitemporal generalized Fisher discriminant vector projection, segment 1681.

32

4. DEVELOPMENT OF ANALYST AIDS

4.1 SEGMENT DEPENDENT PROJECTION RESULTS

For each segment available in the OLPARS data base, the multitemporal Fisher discriminant plane was constructed (see section 1.2) with the acquisitions available. All segments for the years of 1976 and 1977 which are used in this study have at least three acquisitions. The multitemporal Fisher discriminant plane exhibited excellent results when an acquisition on or about julian date 193 was available, and it exhibited acceptable results if an acquisition around the critical day (193) was not available (see section 3.1). In order to define a Fisher plane, ground-truth data are needed for training; therefore, this approach could not be used operationally.

Other planes were studied by using the eigenvectors of the covariance matrix with and without prior data transformation. The eigenvector planes without prior data transformation were extensively analyzed. Notice that segments with four acquisitions define 16 eigenvectors, and hence, 120 different eigenvector planes are possible.

A large number of these planes were observed for potential sources of visual aids for the analyst. Unfortunately, the segment-dependent eigenvector planes did not offer good possibilities for showing separation between spring wheat and barley. These projection planes were not consistent from segment to segment. Also, for a given segment, the eigenvector plane was very sensitive to small changes in the data; i.e., the removal of an outlier made substantial changes to the eigenvector plane. This result is not surprising (ref. 5) given the fact that the variance/covariance matrix is ill-conditioned (see section 4.2).

4.2 FIXED PROJECTION RESULTS

Ideally, it is desirable to have a pair of vectors that define a projection plane in such a way that the separability between spring wheat and barley, and possibly oats, is enhanced. Furthermore, we would hope that this plane is adequate for all segments in the U.S. Great Plains.

The first approach taken to obtain a projection plane that would meet the above requirements was to compute an "average" Fisher plane. First, the Fisher plane was constructed for each of the 1976 and 1977 segments in the OLPARS data base. Next, a 20-day moving average curve of the Fisher vector component values was computed. For a given point in time (julian date), the curve represents the average Fisher component values, averaged over all the segments having an acquisition within 20 days of the julian date. It was hoped that by having a pair of curves as described above, an average Fisher projection plane could be computed for any segment regardless of its acquisition dates. Unfortunately, the results obtained by using the above procedure are not satisfactory. Among all the possible reasons for the unsatisfactory results obtained with the above approach, the most important one deals with the condition number of the pooled covariance matrix. The condition number of a matrix W is the ratio of the largest to the smallest singular value of W , where the singular values are the positive square roots of the eigenvalues of W . Let $\lambda_1 < \lambda_2 < \dots < \lambda_p$ be the eigenvalues of W and v_1, v_2, \dots, v_p be their corresponding orthonormal eigenvectors. It can be shown that for

$$V = [v_1, v_2, \dots, v_p]$$

and

$$L = \text{diag}(\lambda_i)$$

W can be expressed as (ref. 6):

$$W = VLV^T = \sum_{i=1}^p \lambda_i v_i v_i^T$$

Likewise,

$$W^{-1} = \sum_{i=1}^p \lambda_i^{-1} v_i v_i^T$$

Therefore, if the symmetric matrix W is near singular, i.e., ill-conditioned, then the computation of W^{-1} is highly unstable because some of the eigenvalues

λ_i are small. The instability can be shown with a simple numerical example. To solve a system of equations suppose:

$$X\underline{b} = \underline{c}$$

where X is a 2×2 matrix, and \underline{b} and \underline{c} are 2×1 vectors. Obviously, the solution vector is given by

$$\underline{b} = X^{-1} \underline{c} = \left[\frac{1}{|X|} \text{adj } X \right] \underline{c}$$

Let

$$X = \begin{bmatrix} 1.0 & 3.0 \\ 2.00001 & 6.00002 \end{bmatrix}, \quad \underline{c} = \begin{bmatrix} 1.0 \\ 2.0 \end{bmatrix}$$

then \underline{b} is

$$\underline{b} = \frac{1}{-0.00001} \begin{bmatrix} 6.00002 & -3.0 \\ -2.00001 & 1.0 \end{bmatrix} \begin{bmatrix} 1.0 \\ 2.0 \end{bmatrix}$$

$$\underline{b} = \begin{bmatrix} -2.0 \\ 1.0 \end{bmatrix}$$

Now, observe the change in the solution vector \underline{b} if the matrix X is altered slightly. Let

$$X = \begin{bmatrix} 1.0 & 3.0 \\ 1.99997 & 5.99990 \end{bmatrix}$$

Then

$$\underline{b} = \frac{1}{-0.00001} \begin{bmatrix} 5.99990 & -3.0 \\ -1.99997 & 1.0 \end{bmatrix} \begin{bmatrix} 1.0 \\ 2.0 \end{bmatrix}$$

Hence

$$\underline{b} = \begin{bmatrix} 10.0 \\ -3.0 \end{bmatrix}$$

Notice that \underline{b} has changed dramatically due to a change in the fifth decimal place in two entries of the X -matrix.

To compute the Fisher plane, it is necessary to compute the inverse of the pooled covariance matrix. Since the covariance matrix is ill-conditioned,

the Fisher discriminant vectors are highly instable; a small perturbation in the covariance matrix can cause a large change in the Fisher directions. Therefore, the variance of the individual components is high. Hence, the average of the components is highly unreliable. It is believed that this numerical instability of the inverse of W contributed to the inadequate results obtained with the 20-day moving average Fisher plane.

The next approach taken was to select a small number of segments from a stratum. These segments were required to have acquisition dates that were close among the segments. Only three segments met the above requirements. The segments were from stratum 20, and they were 1512 (77), 1830 (77), and 1899 (77). The acquisitions used were on julian dates 157 and 193. Data from these three segments were pooled and then used to compute a Fisher plane. It was expected that this plane would be adequate for all segments from stratum 20 for which acquisitions on or about days 157 and 193 were available. These days correspond to Robertson biostages between 4.0 to 4.9 and 5.0 to 5.9 (see section 3). The vectors that define the above Fisher plane, called the Two-day Fisher plane, are:

$$\text{fsh2x} = [-0.3135, -0.30116, -0.026563, 0.0034115, \\ -0.88881, -0.022443, -0.093723, -0.10508]$$

$$\text{fsh2y} = [-0.010688, -0.01539, -0.10796, 0.12693, \\ 0.079135, -0.89856, -0.37923, -0.12001]$$

It should be noted that oats and wheat were combined into one class in order to find the Fisher plane.

In addition to the Fisher plane, the generalized discriminant projection plane was computed from the pooled data. As mentioned previously, the Fisher plane is defined by two classes or two groups of classes and the generalized discriminant plane is defined by two or more classes or groups of classes. Since the three segments used above contain three classes: wheat, oats, and barley, these two planes are not necessarily the same.

The vectors that define the generalized discriminant plane are:

$$\text{gndv2x} = [0.68189, -0.55583, 0.09401, -0.20383, \\ 0.34103, 0.16443, 0.092563, 0.15422]$$

$$\text{gndv2y} = [0.16339, -0.03512, 0.19668, -0.43773, \\ -0.82202, 0.15419, -0.1147, 0.1728]$$

Figures 4-1 and 4-2 present typical results of using the generalized discriminant plane and the Fisher plane, respectively. These two figures correspond to the projection of segment 1513 (76). Figures 4-3 and 4-4 present similar results for segment 1742 (76).

Following the same rationale used in constructing the Two-day Fisher plane, a One-day Fisher plane was constructed. In section 3, it is established that there exists a best time for separation between wheat and barley. This time corresponds to a Robertson biostage for spring wheat between 5.0 and 5.9 (or around julian date 193).

The data for acquisition 192 from segments 1512 (77), 1830 (77), and 1899 (77) were pooled, and a Fisher plane was obtained. This plane is defined by the vectors

$$3\text{segx} = [-0.97127, -0.057665, -0.10266, -0.20682]$$

and

$$3\text{segy} = [-0.090201, -0.86413, -0.49131, 0.061208]$$

The results obtained by using this One-day Fisher plane, call it 192Fisher, are very encouraging from a signature extension point of view. These projection results were compared with the greenness-brightness (G-B) projection results. The G-B plane is defined by the vectors (ref. 7):

$$\text{Brightness} = [0.433, 0.632, 0.586, 0.264]$$

$$\text{Greenness} = [-0.290, -0.562, 0.600, 0.491]$$

The rationale for using the G-B plane for comparison is that the G-B is presently being used by the Classification and Mensuration Subsystem (CAMS) in an operational mode.

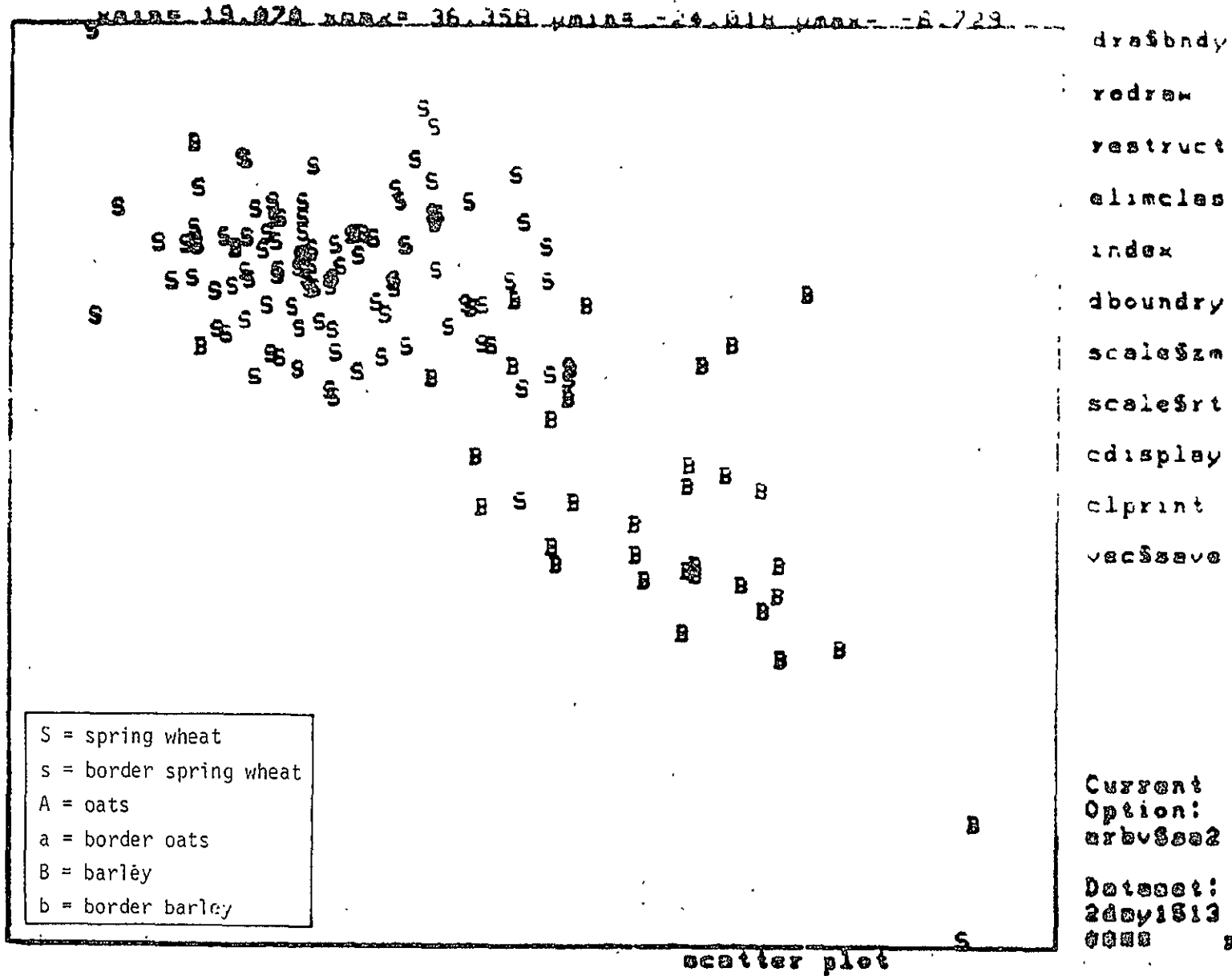


Figure 4-1. Two date generalized Fisher discriminant vector fixed projection, segment 1513.

4-7

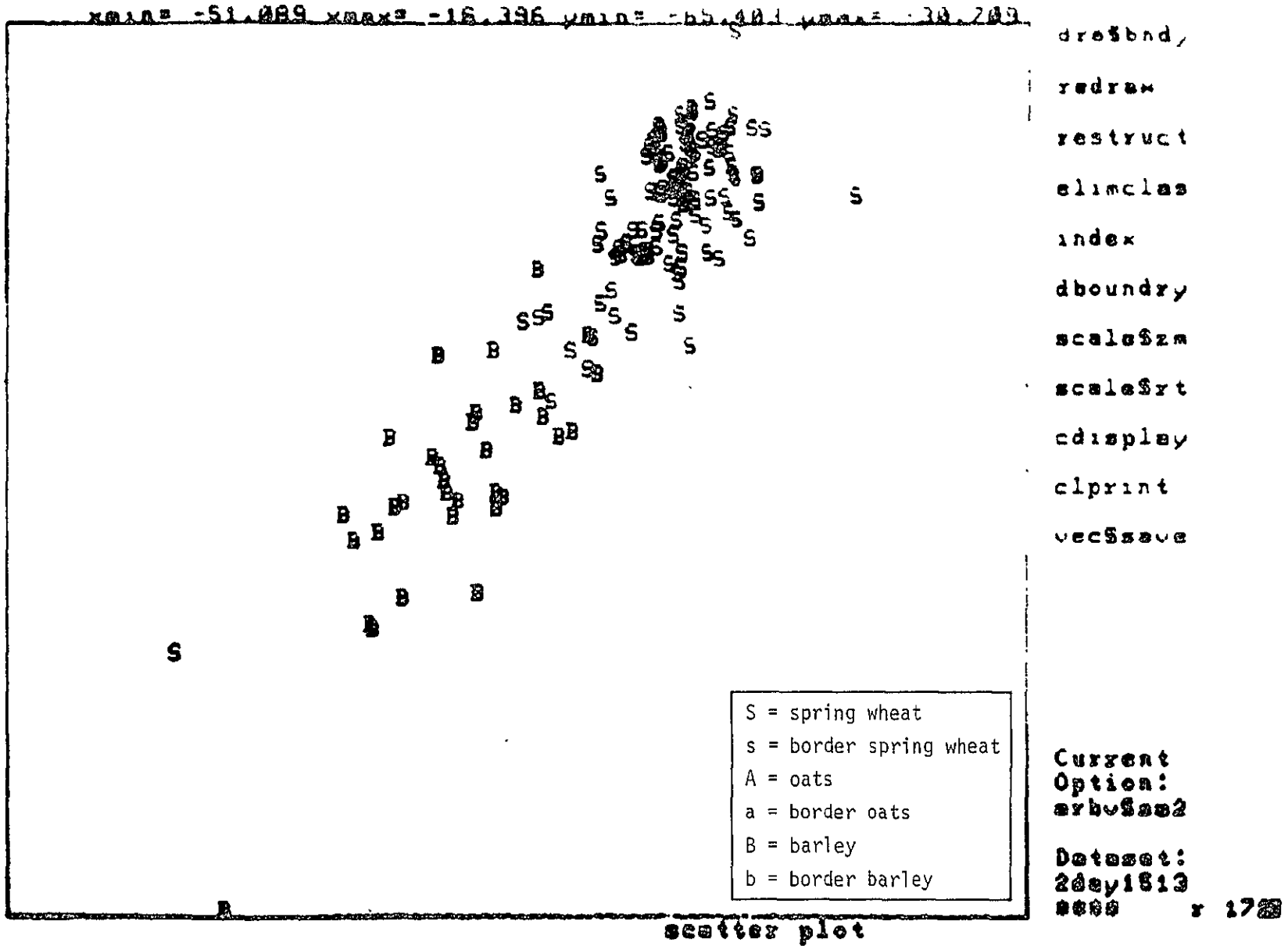
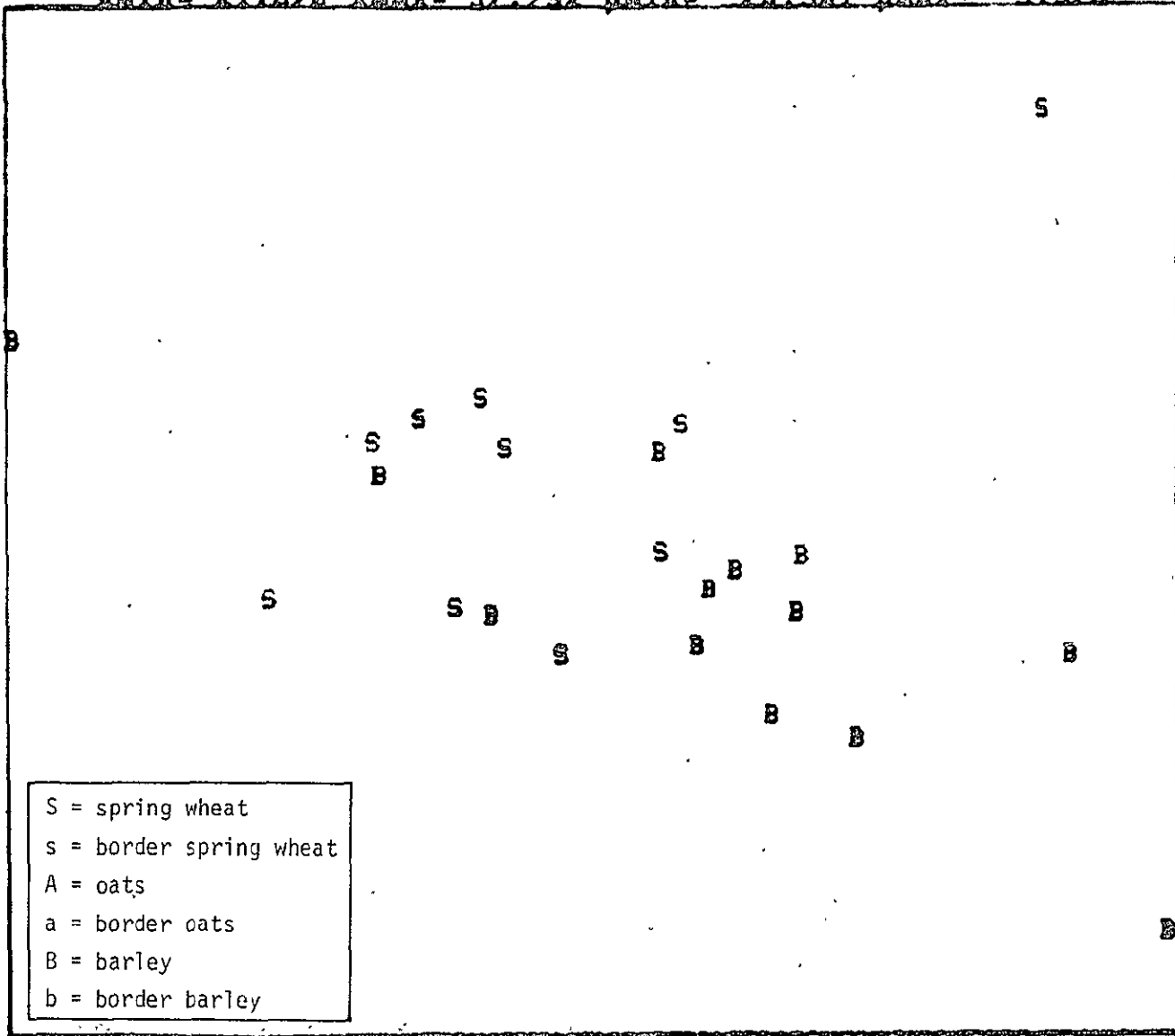


Figure 4-2.— Two date Fisher discriminant vector fixed projection, segment 1513.

width= 21.870 height= 37.792 xmin= -25.301 xmax= -9.329



drawbody
 redraw
 restruct
 eliasies
 index
 dboundary
 scalesm
 scalesrt
 display
 clprint
 versave

Current
 Option:
 arbv8002

Dataset:
 2day1742
 0000 r 170

ORIGINAL PAGE IS
 OF POOR QUALITY

4-8

140

Figure 4-3. Two date generalized Fisher discriminant vector fixed projection, segment 1742.

4-9

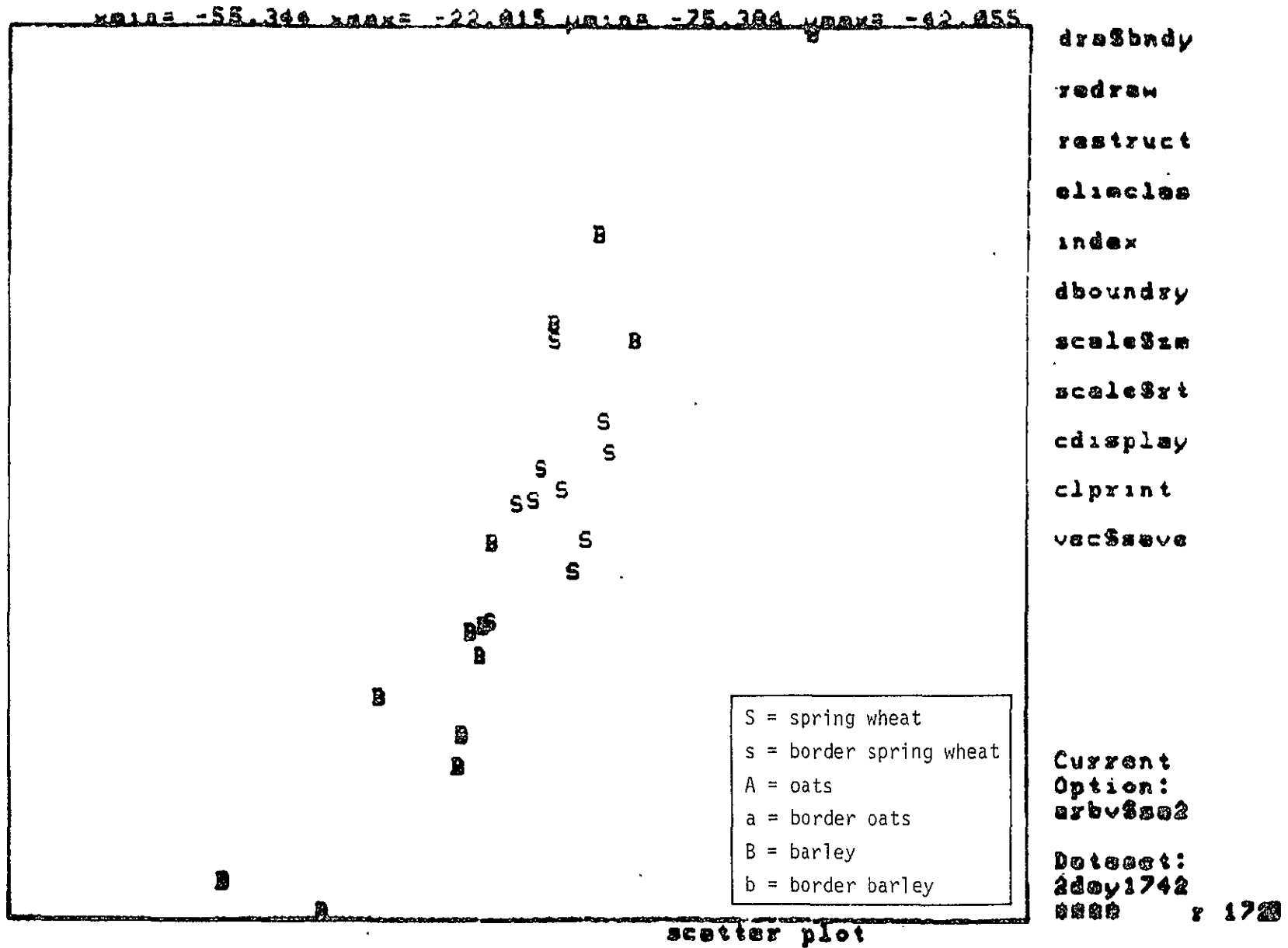


Figure 4-4.— Two date Fisher discriminant vector fixed projection, segment 1742.

Figures 4-5 and 4-6 depict the 192Fisher and G-B projections of segment 1513 (77), acquisition date 193.

The PCC was computed for both types of projections. Two different techniques were used to compute the PCC's. One technique was the NMV classifier and the other was the Fisher pairwise classifier. Table 4-1 presents the value of the overall PCC's for five segments. Table 4-2 contains the mean and standard deviation of the PCC values.

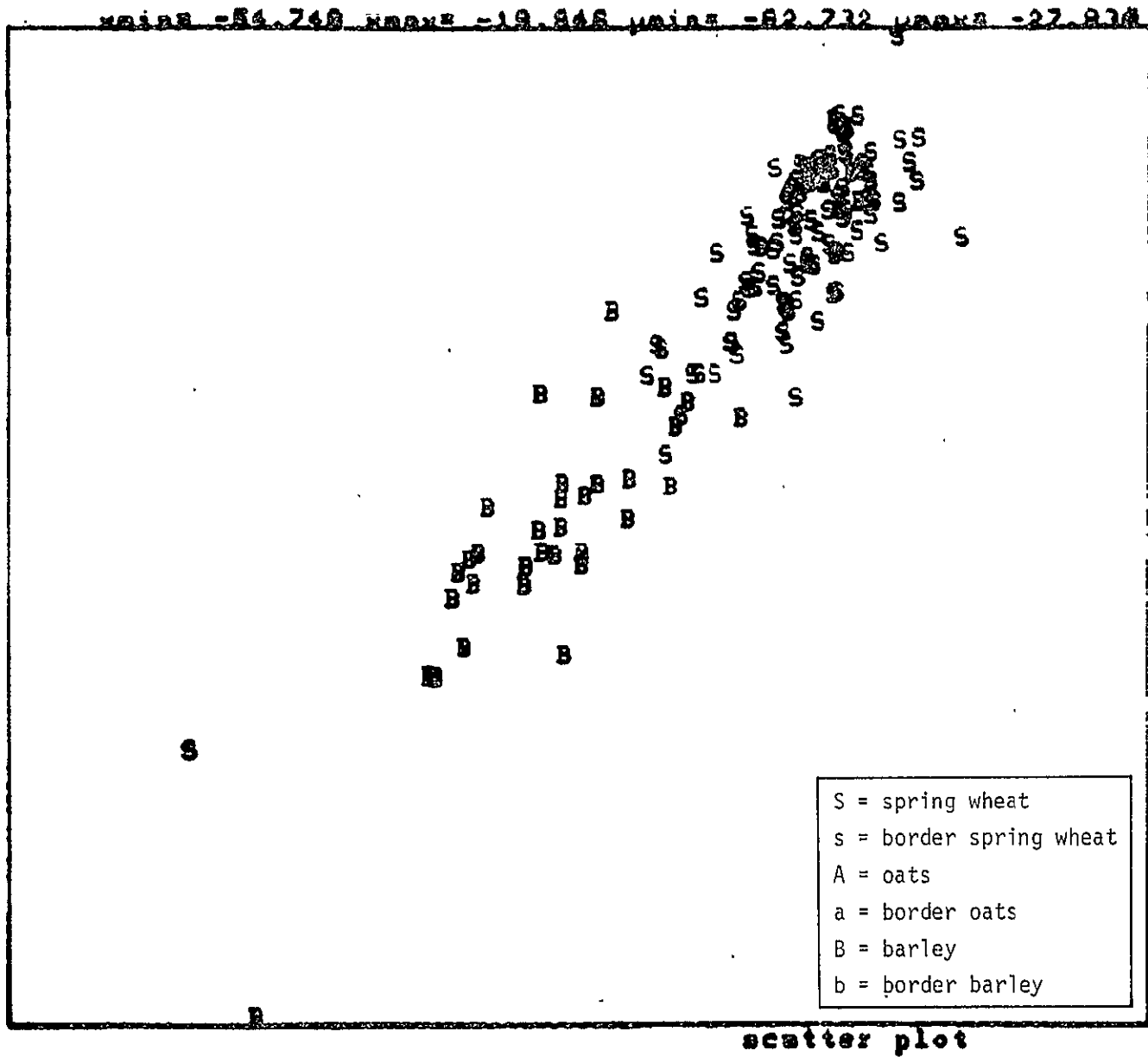
TABLE 4-1.— COMPARISON OF PCC'S FOR G-B AND 192FISHER PROJECTION

Evaluation	Projection		Segment
	G-B	192Fisher	
Fisher	57.14	57.14	1681
NMV	48.21	51.79	Oats, barley, and spring wheat
Fisher	85.71	80.36	^a 1681
NMV	91.07	78.57	Oats-spring wheat and barley
Fisher	93.57	92.86	1513
NMV	89.29	90.71	Barley and spring wheat
Fisher	65.22	60.87	1742
NMV	91.30	65.22	Barley and spring wheat
Fisher	61.36	70.46	1929
MNV	45.46	59.08	Barley and spring wheat
Fisher	64.10	87.18	1614
NMV	71.80	82.05	Wheat and barley

^aOats and wheat were combined into one class.

TABLE 4-2.-- MEAN AND STANDARD DEVIATIONS OF G-B AND 192FISHER PROJECTIONS

Evaluation	Projections	
	G-B	192FISHER
Fisher	Mean: 71.183	Mean 74.812
	Standard deviation: 14.776	Standard deviation: 14.388
NMV	Mean: 72.855	Mean: 71.237
	Standard deviation: 21.453	Standard deviation: 14.914



dresbody
 redres
 restruct
 eliacas
 index
 dboundary
 scalesm
 scalesrt
 edisplay
 clprint
 versave

ORIGINAL PAGE IS
OF POOR QUALITY

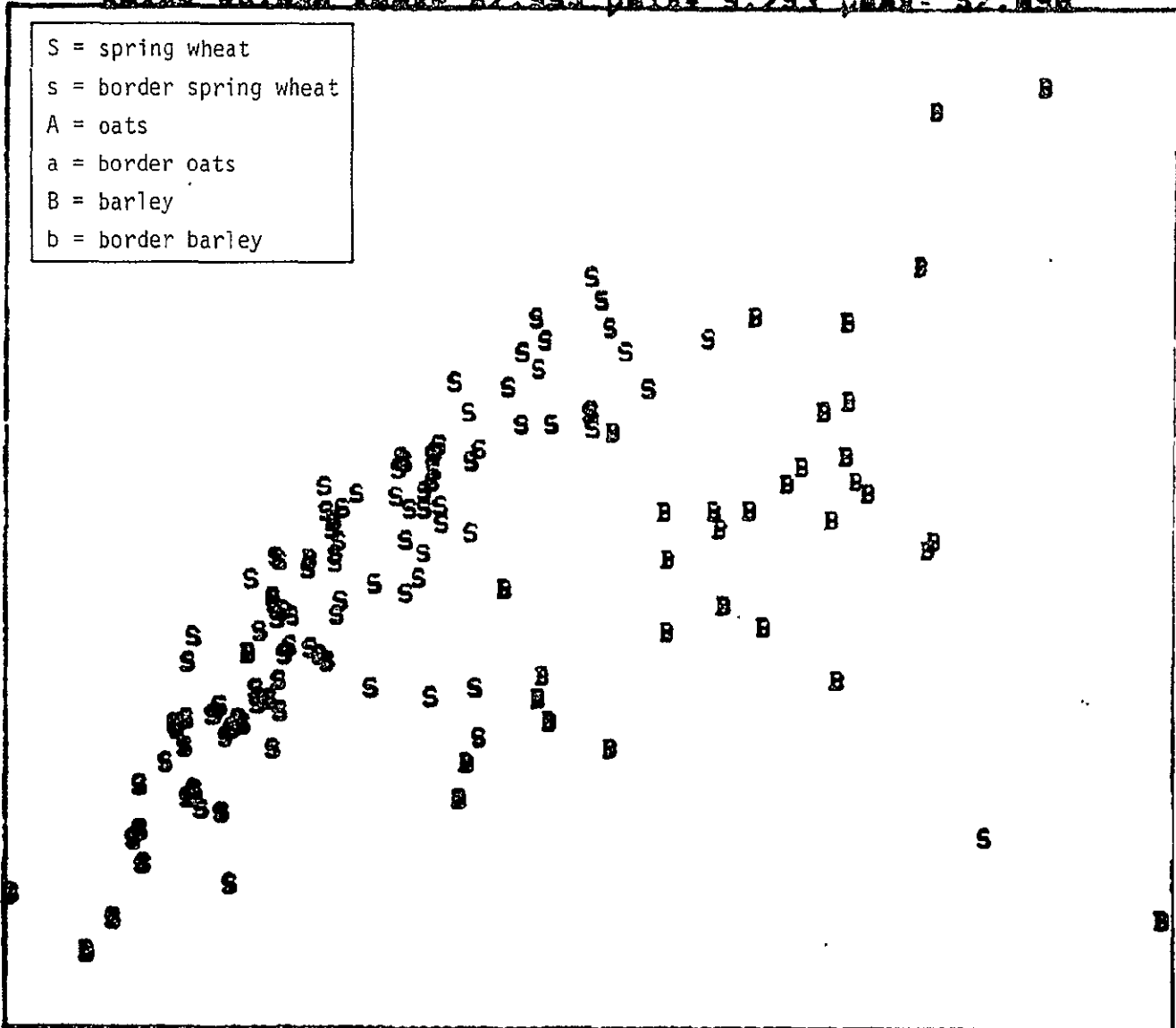
Current
 Option:
 orbv8e2
 Dataset:
 1021513
 ***** r 17

Figure 4-5.— Single date Fisher discriminant vector fixed projection, segment 1513.

57

min= 45.898 max= 87.995 min= 9.793 max= 52.898

S = spring wheat
s = border spring wheat
A = oats
a = border oats
B = barley
b = border barley



```

drawbody
redraw
restruct
elimclass
index
seq
dboundary
scalex
scaley
display
print
erase

```

```

Current
Option:
erase

```

```

Dataset:
1513

```

ORIGINAL PAGE IS
OF POOR QUALITY

4-14

16

projected on axes. 7 and 8 scatter plot

Figure 4-6.— Single date G-B projection, segment 1513.

5. CONCLUSIONS AND RECOMMENDATIONS

5.1 CONCLUSIONS

The conclusions of this study are as follow:

- a. Barley shows significant separability from spring wheat, both multitemporally and on a single date chosen near the turning time for barley (Robertson biostage 5.3 to 5.8 for spring wheat).
- b. Oats show occasional multitemporal separability from barley and spring wheat; however, the cause of this separability is not well understood. Oats show no significant separability from spring wheat on any single date during the growing season.
- c. By pooling data from segments having an acquisition near the turning time for barley, a fixed unitemporal projection for aiding in the labeling of barley versus spring wheat and oats has been constructed. This projection has about the same separability of barley from spring wheat and oats as does the unitemporal greenness versus brightness plot. However, the new fixed projection has the advantage that barley occurs consistently in the same general location on the plot with respect to spring wheat and oats.
- d. Attempts to construct a fixed multitemporal or a segment-dependent multitemporal projection for aiding in the labeling of spring wheat versus other small grains have been unsuccessful due to segment variability and the fact that each segment has a unique acquisition history.

5.2 RECOMMENDATIONS

It is recommended that the fixed unitemporal projection developed during this study be further evaluated in a semioperational setting for its utility in aiding analyst labeling of barley versus spring wheat and oats. In addition, the data set resident on the OLPARS should be expanded and updated to allow more detailed study of wheat-oats separability and to aid in the development of any multitemporal labeling aids.

6. REFERENCES

1. Sammon, J. W., Jr.: Interactive Pattern Analysis and Classification. Trans. IEEE Computers, vol. C-19, July 1970, pp. 594-616.
2. Kanal, Laveen N.: Interactive Pattern Analysis and Classification System: A Survey and Commentary. Proc. IEEE, vol. 60, No. 10, Oct. 1972. pp. 1200-1215.
3. Simmons, E. J., Jr.: Interactive Pattern Recognition - A Designers Tool. Proc. AFTPS, Conference Proceedings, vol. 42, June 1973, pp. 479-483.
4. Connell, David B.; Jackson, Richard A.; and Klingbail, Kermit N.: MULTICS OLPARS Operating System. Report Number RADC-TR-76-271, vol. 1, Rome Air Development Center, Griffis Air Force Base (N. Y.), Sept. 1976.
5. Gnanadesikan, R.: Methods for Statistical Data Analysis of Multivariate Observations. John Wiley & Sons, Inc. (N.Y.), 1977.
6. Seber, G. A. F.: Linear Regression Analysis. John Wiley & Sons, Inc. (N.Y.), 1977.
7. Kauth, R. J.; and Thomas, G. S.: The Tasselled Cap - A Graphic Description of the Spectral-Temporal Development of Agricultural Crops as Seen by Landsat. Proc. Symp., Machine Processing of Remotely Sensed Data, Purdue Univ., June 29-July 1, 1976.

